WILEY-VCH

Omar M. Yaghi, Markus J. Kalmutzki,
and Christian S. Diercks

Introduction to Reticular Chemistry

Metal-Organic Frameworks and Covalent Organic Frameworks

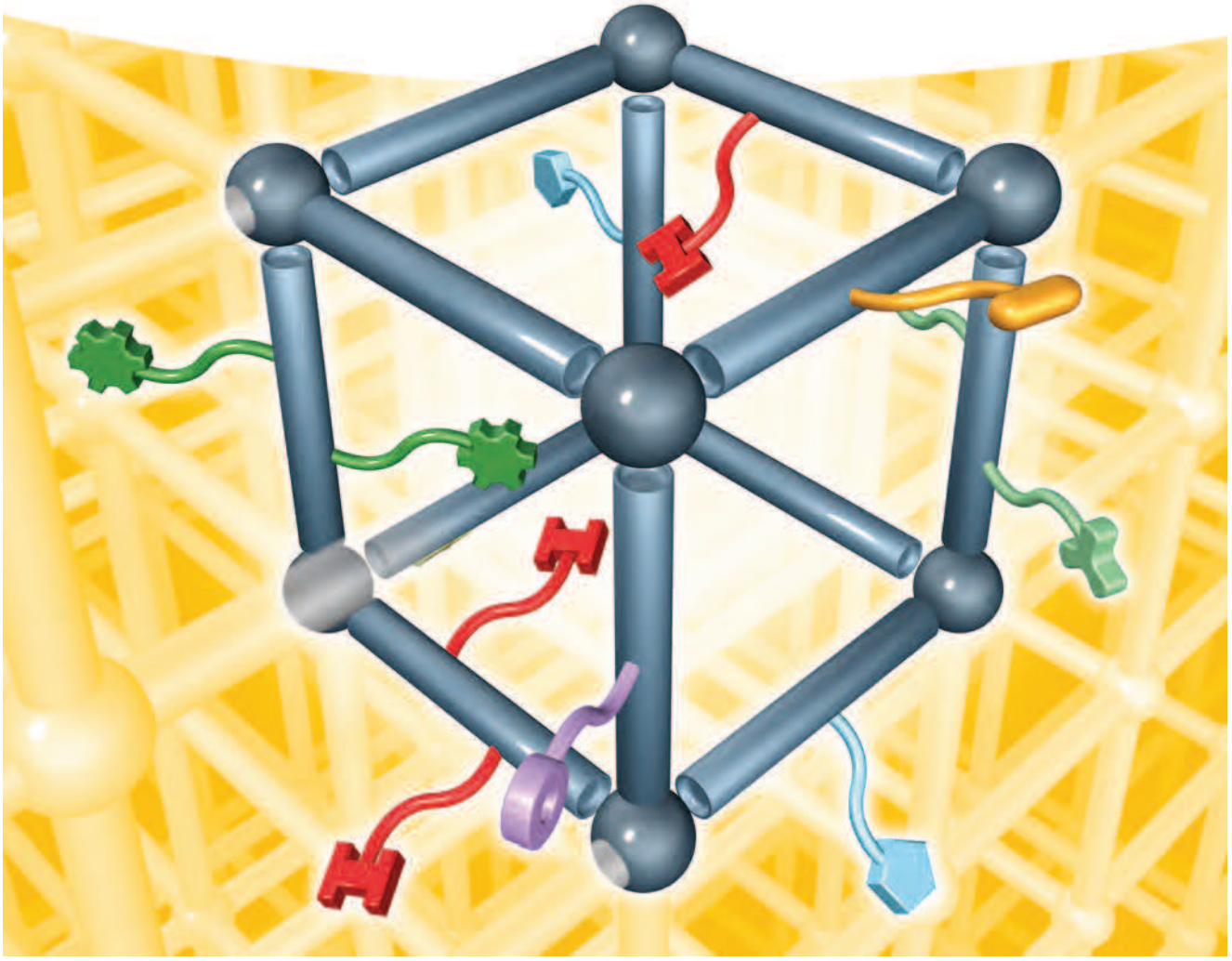

Introduction to Reticular Chemistry

Introduction to Reticular Chemistry

Metal-Organic Frameworks and Covalent Organic Frameworks

Omar M. Yaghi
Markus J. Kalmutzki
Christian S. Diercks

WILEY-VCH

Authors

Prof. Omar M. Yaghi
University of California, Berkeley
Department of Chemistry
602 Latimer Hall
94720 Berkeley, CA
United States

Dr. Markus J. Kalmutzki
University of California, Berkeley
Department of Chemistry
618 Latimer Hall
94720 Berkeley, CA
United States

Christian S. Diercks
University of California, Berkeley
Department of Chemistry
618 Latimer Hall
94720 Berkeley, CA
United States

Library of Congress Card No.:
applied for

British Library Cataloguing-in-Publication Data
A catalogue record for this book is available from the British Library.

Bibliographic information published by the Deutsche Nationalbibliothek
The Deutsche Nationalbibliothek lists this publication in the Deutsche Nationalbibliografie; detailed bibliographic data are available on the Internet at http://dnb.d‐nb.de.

Print ISBN: 978-3-527-34502-1
ePDF ISBN: 978-3-527-82108-2
ePub ISBN: 978-3-527-82110-5
oBook ISBN: 978-3-527-82109-9

Cover Design Formgeber, Mannheim, Germany
Typesetting SPi Global, Chennai, India
Printing and Binding

Printed on acid-free paper

10 9 8 7 6 5 4 3 2 1

To emerging scholars whose curiosity and power of observation make Nature reveal itself

Contents

About the Companion Website

This book is accompanied by a companion website:

http://www.wiley.com/go/yaghi/reticular

The Instructor Companion Site includes:

1) **Figures**
2) **Diamond files**

The provided *.diamdoc files can only be viewed using the crystal structure visualization software DIAMOND: http://www.crystalimpact.de/diamond/Default.htm.

Foreword

Our knowledge of how atoms are linked in space to make molecules and how such molecules react has now reached a sophisticated level leading not only to the formation of useful crystalline materials but also in deciphering important disciplines (e.g. chemical biology, materials chemistry), where chemistry plays an indispensable role in understanding matter. In contrast, the science of making and studying extended chemical structures has remained relatively untouched by the tremendous progress being made in molecular chemistry. This is because solid-state compounds are usually made at high temperatures where the structures of organics and metal complexes do not survive and where their molecular reactivity is not retained. Although this has led to useful inorganic solids being made and studied, the need for translating organic and inorganic complex chemistry with all its subtleties and intricacies into the realm of solid state continued until the end of the twentieth century. At that time, it became clear that the successful synthesis and crystallization of metal-organic frameworks (MOFs) and later covalent organic frameworks (COFs) constituted an important step in developing strong covalent bond and metal–ligand bond chemistry beyond the molecular state. MOFs of organic carboxylates linked to multi-metallic clusters were shown to be architecturally robust and proven to have permanent porosity. Both are critical factors for carrying out precision organic reactions and metal complexations within solid-state structures. With COFs, their successful synthesis and crystallization ushered in a new era for they extended organic chemistry beyond molecules (0D) and polymers (1D) to layered (2D) and framework (3D) structures. The fact that both MOFs and COFs are made under mild conditions, which preserve the structure and reactivity of their building blocks, and that their building blocks are made entirely from strong bonds and are also linked to each other by strong bonds to make crystals of porous frameworks, gave rise to a new thinking in chemistry. By knowing the geometry of the building blocks it became possible to design specific MOF and COF structures, and by knowing the conditions under which such structures formed it became possible to expand their metrics and functionalize their pores without affecting their crystallinity or underlying topology. This is completely new in solid-state chemistry. On the fundamental level, MOFs and COFs represent whole new classes of materials and the intellectual aspects of their chemistry provided a new thinking for the practicing scientist. One might go as far as to say that this new chemistry, termed reticular

chemistry, gave credence to the notion of materials on demand. At present, reticular chemistry is being practiced and researched in over a thousand laboratories around the world in academia, industry, and government. The utility of reticular materials in many fields such as gas adsorption, water harvesting, and energy storage, to mention a few, makes this new field all the more interesting to explore and teach since it covers aspects from basic science to real world applications. Accordingly, we have endeavored in this book to provide an introductory entry into this vast field. The book is divided roughly into four parts, which are seamlessly joined in their presentation. The first part (Chapters 1–6) focuses on MOF chemistry and presents their synthesis, building blocks, characterization, structures, and porosity. The second part (Chapters 7–11) presents COF chemistry in a sequence similar to that of MOFs but with emphasis on the organic chemistry used to produce their linkers and linkages. The third part (Chapters 12–17) is dedicated to the applications of MOFs with some mention of those pertaining to COFs. Here, we have endeavored to give a basic description of the physical principles for each application and how reticular materials are deployed. The fourth part (Chapters 18–21) is what we have referred to as special topics that are related to reticular chemistry thinking and analysis. The book is written to allow instructors to use each part independently from the others, and for most chapters, they can also be taught out of sequence or even separately. We hope the students and instructors will appreciate through this textbook that reticular chemistry as a field of study is rooted in organic, inorganic, and physical chemistry, and that it has merged these traditional disciplines into one to produce useful crystalline materials without losing the precision of molecular chemistry. The book is unique in its coverage of the basic science leading to the synthesis, structure, and properties as well as to the applied science of using these materials in addressing societal challenges. Reticular chemistry extends molecular chemistry and its precision in making and breaking bonds to solid-state framework structures being linked by strong bonds. It is now realistic to think in the following way: what the atom is to the molecule, the molecule is to the framework. The molecule fixes the atom in a specific orientation and spatial arrangement, while the framework fixes the molecule into specific orientation and spatial arrangement; except that the framework also encompasses space within which matter can be further manipulated and controlled. It is a new field that combines the beauty of chemical structures, chemistry of building units and their frameworks, and relevance to societal challenges. We have sought to communicate these aspects in our book to provide a rich and stimulating arena for learning.

Berkeley
March 2018

Markus J. Kalmutzki
Christian S. Diercks
Omar M. Yaghi

Acknowledgment

The authors wish to thank the following scholars from the Yaghi research group at the University of California, Berkeley, who contributed selflessly to proofreading of the manuscript: Dr. Eugene Kapustin, Mr. Kyle Cordova, Mr. Robinson Flaig, Mr. Peter Waller, Mr. Steven Lyle, and Dr. Bunyarat Rungtaweevoranit.

We also wish to express our gratitude for the commitment and extensive efforts of Ms. Paulina Kalmutzki, who lent her precious time to the Yaghi group, and Dr. Yuzhong Liu (Yaghi group) for help with the preparation of illustrations. We want to acknowledge Prof. Adam Matzger (University of Michigan), Dr. Bunyarat Rungtaweevoranit, and Yingbo Zhao (Yaghi group) for providing some of the microscopy images found in this text.

Finally, we would like to thank our publisher, Wiley VCH Weinheim, especially Anne Brennführer and Sujisha Karunakaran, for the understanding and assistance provided throughout all stages of the elaborate and laborious task of producing this book.

Introduction

Reticular Chemistry is concerned with making and breaking bonds in molecules and how this can be done in a controlled fashion. When a new molecule is discovered, the need and desire to build it up from simple starting materials using logical means becomes a central objective. Thus, chemists first and foremost are architects and builders: generally, a "blueprint" for a target molecule is designed and a reaction pathway is determined for making it. Often, this blueprint also includes a strategy for achieving the desired molecular geometry and spatial arrangement of atoms, as these dramatically impact the properties of molecules. This sequence of operations is so well developed in organic chemistry that virtually any reasonable target can be designed and made with high precision. The deliberate chemical synthesis approach thus employed is less developed for metal complexes because a metal ion can adopt different geometries and coordination numbers thereby introducing uncertainty into the outcome of the synthesis. Furthermore, unlike organic molecules, where multiple chemical reactions can be carried out to functionalize them, metal complexes are modified largely by substitution–addition reactions. This is because of the limitations imposed by the chemical stability of metal complexes. Thus, the step-by-step approach to the synthesis of organic compounds is severely limited in the synthesis of metal complexes, and this adds a significant component of trial-and-error to metal ion chemistry. It should be noted that the uncertainty in metal-complex chemistry is sometimes obviated by sophisticated design of multi-dentate organic ligands, whereby a metal ion can be locked into a specific geometry and coordination mode. It remains, however, that although immense diversity can be created, the ability to control the geometry around the metal ion and spatial arrangement of ligands is an ongoing challenge.

A new level of precision and control in chemical synthesis is achieved when linking molecules together to make larger discrete and extended structures. There are two basic aspects to consider in linking molecules: the first pertains to the type of interactions used in such linkages and the directionality they impart to the formation of the resulting structure, and the second is concerned with the geometry of the molecular building units and how their metric characteristics such as length, size, and angles guide the synthesis to a specific structure. These aspects are at the core of reticular chemistry, which is concerned with linking molecular building units by strong bonds to make crystalline large and extended structures.

Reticular chemistry started by linking metal ions through strong bonds using charged organic linkers such as carboxylates leading to metal-organic

frameworks (MOFs) and related materials. These frameworks in effect expanded the scope of inorganic complex chemistry to include extended structures in which the building units are fixed in precise geometrical and spatial arrangements. Another development was to extend organic chemistry beyond molecules and polymers by using reticular chemistry to link organic building blocks into crystalline two- and three-dimensional covalent organic frameworks (COFs).

The subject of reticular chemistry is also concerned with providing a logical framework for using molecular building units to make structures with useful properties. The concept of node and link that was introduced by Alexander F. Wells to describe a net (collection of nodes and links) has become central to the "grammar" and "taxonomy" of reticular structures, which we discuss in this book. They encompass both, large discrete entities such as metal-organic polyhedra (MOPs) and covalent organic polyhedra (COPs) and extended frameworks such as MOFs, zeolitic imidazolate frameworks (ZIFs), and COFs. This field expanded dramatically and has come to represent a significant segment of the larger field of chemistry.

Among the extensive body of knowledge produced from linking building units using reticular chemistry there are a number of challenges that have been addressed: First, the propensity of metal ions to have variable coordination number and geometries, as mentioned above, is detrimental to controlling the outcome of linking metal ions with organic linkers into MOFs or MOPs. Although exceptions may be found where a metal ion prefers a specific arrangement such as square planar for divalent platinum, in general the use of single metal ions as nodes detracts from the needed control in producing a specific structure. The use of poly-nuclear complexes named secondary building units (SBUs), as in metal carboxylate clusters, locks the metal ions into position and thereby the coordination geometry of the entire SBU is the determining factor in the reticulation process. Second, since the SBUs are clusters by necessity and the organic linkers are multi-atomic, reticular synthesis inevitably yields open structures. The fact that the SBUs are rigid and directional provides for the possibility of design and control of the resulting material. Since the SBUs are made of strong bonds, when joined by organic linkers, they ensure architectural stability and permanent porosity of the framework when the molecules filling its pores are removed. The strong bonds also impart thermal stability and, when they are kinetically inert, chemical stability of the overall porous structure. Third, the ability to determine the conditions under which a specific SBU forms has led to isoreticular synthesis where the same SBU can be joined by a variety of linkers having the same linkage modality but with different size, length, and functional groups attached to them. Fourth, the discovery of the conditions to crystallize the products of these reticular syntheses has enabled the definitive characterization of the outcome of the structures by X-ray diffraction and has facilitated structure–property relationships. Ultimately, this aspect has vastly contributed to the design of structures with specific functionality and pore metrics. Fifth, the permanent porosity, thermal and chemical stability, and crystallinity of these frameworks allow for chemical modification to be carried out on their interior with full preservation of porosity and crystallinity. This meant that large and extended structures can be transformed post-synthetically, and

that the incorporation of a specific functionality can be achieved either before or after formation of the product. Sixth, the precision with which such frameworks can be made and their interior modified coupled to the flexibility in deploying a variety of SBUs and organic linkers to make metal-organic and organic reticular materials have given rise to a vast number of properties and applications.

Reticular chemistry has advanced to the point where flexibility and dynamics can be incorporated into large and extended structures. This is accomplished by using flexible constituents or by introducing mechanically interlocking rings within the organic linker. More recently, mechanical entanglement was successfully used in interlacing organic threads to make woven extended structures. In principle, this strategy is also applicable to the interlocking of large discrete rings.

To fully appreciate reticular chemistry and its potential, it is instructive to view reticular structures as being composed of backbone, functionality attached to the backbone, and space encompassed by this construct. The backbone provides the overall structural integrity while the functionality provides for optimal pore environment. The pores can be adjusted to allow for molecules of various sizes, shapes, and character to be incorporated and potentially transformed. In cases when multiple functionalities are used to decorate the pores, the possibility of having unique sequences of chemical entities becomes a reality and the potential for such sequences to code for specific properties exists. The diffusion of molecules within such pore space will undoubtedly be influenced by the specific sequence. This ushers a new era in chemistry where it becomes possible to design and make sequence-dependent materials. The recent advance in "editing" reticular structures by linker or metal substitution without changing the overall porosity and order within the structure is a very promising direction for being able to deliberately alter such chemical sequences. It follows from this discussion that reticular structures are amenable to the introduction of heterogeneity such as defects and functionality by design making it possible to target specific reactivity in ways not possible otherwise.

By linking molecules together into large and extended structures, reticular chemistry has in effect endowed the molecule with additional properties inaccessible without it being linked. Specifically, since the molecule in the reticular structure is fixed in position, it becomes more directly addressable, and depending on where it is linked, the units surrounding it can be considered effectively as "protecting groups." The fact that molecules are repeated throughout the structure provides opportunities for that molecule to be part of a whole that could function above and beyond the sum of its parts. The interface between the molecules making up the structure and other molecules freely residing in the pores as guests is a well-defined region of the overall structure. This interface is also endowed with the same precision of design and definition that is so characteristic to reticular structures. Accordingly, the interface can be varied and tailored in ways the molecule cannot experience outside this intricate environment. In essence, what reticular chemistry has done is to provide means of controlling matter beyond molecules, in large and extended structures, and to also provide the space within which molecules can be further controlled and manipulated.

Abbreviations

1,2-H_2DACH	1,2-diaminocyclohexane
(V)MIL-47	V(O)(BDC)
^{13}C CP-MAS	^{13}C cross-polarization magic angle spinning
2,6-H_2NDC	naphthalene-2,6-dicarboxylic acid
1,4-H_2NDC	4,4′-(naphthalene-2,6-diyl)dibenzoic acid
2-mBIM	2-methylbenzimidazolate
4,4′-H_2DMEDBA	4,4′-(1,2-dimethoxyethane-1,2-diyl)dibenzoic acid
4-nIM	4-nitroimidazolate
5-BBDC	5-*tert*-butyl-1,3-benzenedicarboxylate
AB	4-aminobenzoate
acac	acetylacetonate
AD	adeninate
ADHP	adsorption-driven heat pumps
ADI	adiponitrile
AFM	atomic force microscope/atomic force microscopy
aIM	2-carbaldehyde imidazolate
Al-PMOF-1	$Al_2(OH)_2$(TCPP-H_2)
Al-soc-MOF-1	$[In_3O(H_2O)_3]_2(TCPT)_3(NO_3)$
ANH	aromatic *N*-heterocycle
APTES	3-aminopropyltriethoxysilane
ASA	*p*-arsanilic acid
ATZ	5-amino-triazolate
BASF	Badische Anilin und Soda Fabrik
BBC	4,4′,4″-(benzene-1,3,5-triyl-tris(benzene-4,1-diyl))tribenzoate
BBCDC	9*H*-carbazole-3,6-dicarboxylate
bBIM	5-bromo-1H-benzo[d]imidazole
bBIM	6-bromobenzimidazolate
BBO-COF-1	$[(TFB)_2(PDA\text{-}(OH)_2)_3]_{benzoxazole}$
BBO-COF-2	$[(TFPB)_2(PDA\text{-}(OH)_2)_3]_{benzoxazole}$
BDA	terephthaldehyde
BDA-(F)	2-fluoroterephthaldehyde
BDA-$(F)_4$	2,3,5,6-tetrafluoroterephthaldehyde

BDA-(H_2C—C≡CH)	2,5-bis(2-propynyloxy)terephthalaldehyde
BDA-$(OH)_2$	2,5-dihydroxy-1,4-benzenedialdehyde
BDA-$(OMe)_2$	2,5-dimethoxyterephthaldehyde
BDBA	1,4-phenylenediboronic acid
BDH-$(OEt)_2$	2,5-diethoxyterephtalohydrazide
BET model	Brunauer–Emmett–Teller model
BIM	benzimidazolate
bio-MOF-100	$[Zn_6O_2(AD)_4(BPDC)_6](NO_3)_4$
bio-MOF-101	$[Zn_6O_2(AD)_4(NDC)_6](NO_3)_4$
bio-MOF-102	$[Zn_6O_2(AD)_4(ABDC)_6](NO_3)_4$
bio-MOF-103	$[Zn_6O_2(AD)_4(NH_2\text{-}TDC)_6](NO_3)_4$
BIPY	4,4′-bpyridine
BLP	1,3,5-(*p*-aminophenyl)-benzene-borane
Boc	*tert*-butyloxycarbonyl
BPDA	4,4′-biphenyldialdehyde
BPEE	(*E*)-1,2-di(pyridin-4-yl)ethene
Br-H_2BDC	2-bromoterephthalic acid
BTB	4,4′,4″-benzene-1,3,5-triyltribenzoate
BTBA	benzene-1,3,5-triyltriboronic acid
BTCTB	4,4′,4″-[benzene-1,3,5-triyltris (carbonylimino)]tris-benzoate)
BTDD	bis(1*H*-1,2,3-triazolo[4,5-*b*],[4′,5′-*i*]) dibenzo[1,4]dioxin
BTE	4,4′,4″-(benzene-1,3,5-triyl-tris(benzene-4,1-diyl))tribenzoate
BTEB	4′,5′-bis(4-carboxyphenyl)-[1,1′:2′,1″-terphenyl]-4,4″-dicarboxylic acid
Bu	butyl
BZD-$(NO_2)_2$	2,2′-dinitrobenzidine
CAL	coordinative alignment
CAU-10	Al(OH)(*m*-BDC)
cBIM	5-chloro-1*H*-benzo[*d*]imidazole
cBIM	6-chlorobenzimidazole
CBP	Cu(I)bis-4,4′-(1,10-phenanthroline-2,9-diyl) diphenol
CCS	CO_2 capture and sequestration
CdIF-4	$Cd(eIM)_2$
CdIF-9	$Cd(nIM)_2$
cIM	2-chloro imidazolate
Cl_2-H_2BDC	2,5-dichloroterephthalic acid
CNG	compression of natural gas
Co(TAP)	tetra(4-aminophenyl)porphinato cobalt
COD	1,5-cyclooctadiene
COF	covalent organic framework
COF-1	$[BDBA]_{boroxine}$
COF-102	$[TBPM]_{boroxine}$
COF-103	$[TBPS]_{boroxine}$

COF-105	$[(TBPS)_3(HHTP)_4]_{boronate\ ester}$
COF-108	$[(TBPM)_3(HHTP)_4]_{boronate\ ester}$
COF-202	$[(TBPM)_3(tert\text{-butylsilane triol})_4]_{borosilicate}$
COF-300	$[(TAM)(BDA)_2]_{imine}$
COF-320	$[(TAM)(BPDA)_2]_{imine}$
COF-366	$[(H_2TAP)(BDA)_2]_{imine}$
COF-366-Co	$[(Co(TAP))(BDA)_2]_{imine}$
COF-367-Co	$[(Co(TAP))(BPDA)_2]_{imine}$
COF-42	$[(TFB)_2(BDH\text{-}(OEt)_2)_2]_{hydrazone}$
COF-43	$[(TFP)_2(BDH\text{-}(OEt)_2)_2]_{hydrazone}$
COF-5	$[(HHTP)_2(BDBA)_3]_{boronate\ ester}$
COF-505-Cu	$(Cu)(BF_4)[(PDB)(BZD)_2]_{imine}$
COP	covalent organic polyhedron
CP-MAS	cross-polarization magic angle spinning
CP-MAS NMR	cross-polarization magic angle spinning NMR
CS-COF	$[(HATP)_2(PT)_3]_{phenazine}$
CTF-1	$[DCyB]_{triazine}$
Cu(TAP)	[5,10,15,20-tetrakis(4-aminophenyl) porphinato]-copper
CuBTTri	$H_3[(Cu_4Cl)_3(BTTri)_8]$
DAA	2,6-diaminoanthracene
DAB	(([2,2′-bipyridine]-5,5′-diylbis(oxy)) bis(4,1-phenylene))dimethanamine
DABCO	1,4-Diazabicyclo[2.2.2]octan
DABCO	1,4-Diazabicyclo[2.2.2]octane
DBA	hexahydroxy-dehydrobenzoannulene
DBS	4-(dodecycloxy)benzoic acid
dcIM	4,5-dichloroimidazolate
DCyB	1,4-dicyanobenzene
DEA	diethylamine
DFP	2,6-pyridinedicarboxaldehyde
DIT	1,14-di-iodo-3,6,9,12-tetraoxy-tetradecane
DLS	dynamic light scattering
DMA	dimethylamine
dmBIM	5,6-dimethylbenzimidazole
DMF	*N*,*N*-dimethylformamide
DMOF	$Zn(BDC)(DABCO)_{0.5}$
DMOF-1(NH_2)	$Zn_2(NH_2\text{-}BDC)_2(DABCO)$
DOBPDC	4,4′-dioxidobiphenyl-3,3′-dicarboxylate
DOE	US Department of Energy
DOX	doxorubicin
DSC	differential scanning calorimetry
DUT	Dresden University of Technology
DUT-32	$Zn_4O(BPDC)(BTCTB)_{4/3}$
DUT-51	$Zr_6O_6(OH)_2(DTTDC)_4(CH_3COO)_2$
DUT-67	$Zr_6O_6(OH)_2(TDC)_4(CH_3COO)_2$
DUT-69	$Zr_6O_4(OH)_4(TDC)_5(CH_3COO)_2$

EDDB	4,40-(ethyne-1,2-diyl)dibenzoic acid
EDX	energy dispersive X-ray spectroscopy
eIM	2-ethyleimidazolate
ElAPO	metal-aluminophosphate with additional Li, Be, B, Ga, Ge, As, Ti
ElAPSO	metal-silicoaluminophosphate with additional Li, Be, B, Ga, Ge, As, Ti
en	1,2-ethylene diamine
Et	ethyl
ETTA	1,1,2,2-tetrakis(4-aminophenyl)ethane
FDM	Fudan Materials
FDM-3	$[(Zn_4O)_5(Cu_3OH)_6(PyC)_{22.5}(OH)_{18}(H_2O)_6][Zn(OH)(H_2O)_3]_3$
FT-IR	Fourier-transform infrared spectroscopy
GCMC	grand canonical Monte Carlo
gea-MOF-1	$Y_9(\mu_3\text{-}OH)_8(\mu_2\text{-}OH)_3(BTB)_6$
GIWAXS	grazing incidence wide angle X-ray scattering
GLU	glutaronitrile
H_2ABDC	(*E*)-4,4′-(diazene-1,2-diyl)dibenzoic acid
H_2ADC	anthracene-9,10-dicarboxylic acid
H_2BATZ	bis(5-amino-1H-1,2,4-triazol-3-yl)methane
H_2BBTA	1*H*,5*H*-benzo(1,2-d:4,5-d′)bistriazole
H_2BDC	terephthalic acid (benzene-1,4-dicarboxylic acid)
H_2BPCu	Cu^{2+}-4,7,10,13,16,19,22,25-octaoxa-2(2,9)-phenanthrolina-1,3(1,4)-dibenzenacyclohexacosaphane @ 4,4′-(1,10-phenanthroline-3,8-diyl)dibenzoic acid
H_2BPDC	[1,1′-biphenyl]-4,4′-dicarboxylic acid
H_2BPyDC	[2,2′-bipyridine]-5,5′-dicarboxylic acid
H_2CBDA	4,4′-carbonyldibenzoic acid
H_2CONQDA	4,4′-(5,6,12,13-tetrachloro-1,3,8,10-tetraoxo-1,3,8,10-tetrahydroanthra[2,1,9-def:6,5,10-d′e′f′]diisoquinoline-2,9-diyl)dibenzoic acid
H_2DMBDA	4,4′-((2,5-dimethoxy-1,4-phenylene) bis(ethyne-2,1-diyl))dibenzoic acid
H_2DTTDC	dithieno[3,2-b:2′,3′-d]thiophene-2,6-dicarboxylic acid
H_2EDBA	(*E*)-4,4′-(ethene-1,2-diyl)dibenzoic acid
H_2HPDC	4,5,9,10-tetrahydropyrene-2,7-dicarboxylic acid
H_2MPBA	4-(3,5-dimethylpyrazol-4-yl)benzoic acid
H_2MPDA	4,4′-(2,9-dimethyl-1,10-phenanthroline-3,8-diyl)dibenzoic acid
H_2NDC	naphthalene-2,6-dicarboxylic acid
H_2OBA	4,4′-oxybis(benzoic acid)

H_2PDC	pyrene-2,7-dicarboxylic acid
H_2TAP	5,10,15,20-tetrakis(4-amino-phenyl)porphyrin
H_2TDC	thiophene-2,5-dicarboxylic acid
H_2TPDC	[1,1′:4′,1″-terphenyl]-4,4″-dicarboxylic acid
H_2TTC	2,2′:5′,2″-terthiophene-5,5″-dicarboxylic acid
H_3BBC	5″-(4′-carboxy-[1,1′-biphenyl]-4-yl)-[1,1′:4′,1″:3″,1‴:4‴,1⁗-quinquephenyl]-4,4⁗-dicarboxylic acid
H_3BHTC	[1,1′-biphenyl]-3,4′,5-tricarboxylic acid
H_3BTB	5′-(4-carboxyphenyl)-[1,1′:3′,1″-terphenyl]-4,4″-dicarboxylic acid
H_3BTC	benzene-1,3,5-tricarboxylate
H_3BTE	4,4′,4″-(benzene-1,3,5-triyltris(ethyne-2,1-diyl)tribenzoic acid
H_3BTN	6,6′,6″-(benzene-1,3,5-triyl)tris(2-naphthoic acid)
H_3BTT	1,3,5-benzetristetrazole
H_3BTTC	benzo[1,2-b:3,4-b′:5,6-b″]trithiophene-2,5,8-tricarboxylic acid
H_3BTTri	1,3,5-tris(1H-1,2,3-triazol-5-yl)benzene
H_3HTB	4-[7,11-bis(4-carboxyphenyl)-2,4,6,8,10,12,13-heptaazatricyclo[7.3.1.05,13]trideca-1,3,5,7,9,11-hexaen-3-yl]benzoic acid
H_3IMDC	1*H*-imidazole-4,5-dicarboxylic acid
H_3TAPB	4′,4‴,4⁗′-(1,3,5-triazine-2,4,6-triyl) tris(([1‴,1⁗′-biphenyl]-4-carboxylic acid))
H_3TATAB	4,4′,4″-((1,3,5-triazine-2,4,6-triyl) tris(azanediyl))tribenzoic acid
H_3TATAB	4,4′,4″-((1,3,5-triazine-2,4,6-triyl) tris(azanediyl))tribenzoic acid
H_3TATB	4,4′,4″-(1,3,5-triazine-2,4,6-triyl)tribenzoic acid
H_3TCA	4,4′,4″-nitrilotribenzoic acid
H_3TCPBA	4′,4‴,4⁗′-nitrilotris(([1‴,1⁗′-biphenyl]-4-carboxylic acid))
H_3TTCA	triphenylene-2,6,10-tricarboxylic acid
H_3TZI	5-tetrazolylisophthalic acid
H_4ABTC	(*E*)-5,5′-(diazene-1,2-diyl)diisophthalic acid
H_4ADBTD	5′,5‴-(anthracene-9,10-diyl) bis(([1,1′:3′,1″-terphenyl]-4,4″-dicarboxylic acid))
H_4ADIP	4,4′-(anthracene-9,10-diyl)dibenzoic acid
H_4ATB	4,4′,4″,4‴-(adamantane-1,3,5,7-tetrayl) tetrabenzoic acid
H_4BBDC	5-boronobenzene-1,3-dicarboxylate

H_4BITC	18-crown-6 @ 4,4′,4″,4‴-(1,4-phenylenebis(1*H*-benzo[d]imidazole-2,4,7-triyl))tetrabenzoic acid
H_4BNETBA-$(OEt)_2$	4,4′,4″,4‴-((1*E*,1′*E*,1″*E*,1‴*E*)-(2,2′-diethoxy-[1,1′-binaphthalene]-4,4′,6,6′-tetrayl) tetrakis(ethene-2,1-diyl))tetrabenzoic acid
H_4BPDCD	9,9′-([1,1′-biphenyl]-4,4′-diyl)bis(9*H*-carbazole-3,6-dicarboxylic acid)
H_4BPTC	[1,1′-biphenyl]-3,3′,5,5′-tetracarboxylic acid
H_4CBI	1,12-Bis(3′,5′-bis(hydroxycarbonyl) phen-1-yl)-1,12-dicarba-closododecaborane
H_4CQDA$(OEt)_2$	5′,5″-bis(4-carboxyphenyl)-2′,2″-diethoxy-[1,1′:3′,1″:3″,1‴-quaterphenyl]-4,4‴-dicarboxylic acid
H_4DH_{11}PhDC/DOT-XI	4′-[4′-(4′-{4′-[4′-(4-carboxy-3-hydroxyphenyl)-2,2′,5,5′-tetramethyl-[1,1′-biphenyl]-4-yl]-5′-hexyl-2,5-dimethyl-2′-pentyl-[1,1′-biphenyl]-4-yl}-2,2′,5,5′-tetramethyl-[1,1′-biphenyl]-4-yl)-2,5-dimethyl-2′,5′-dipentyl-[1,1′-biphenyl]-4-yl]-3-hydroxy-2′,5′-dimethyl-[1,1′-biphenyl]-4-carboxylic acid
H_4DOT	2,5-dihydroxyterephthalic acid
H_4DOT-III	3,3″-dihydroxy-2′,5′-dimethyl-(1,1′:4′,1″-terphenyl)-4,4″-dicarboxylic acid
H_4ETTC	4′,4‴,4⁗,4⁗′,4⁗″-(ethene-1,1,2,2-tetrayl) tetrakis(([1,1′-biphenyl]-4-carboxylic acid))
H_4MTB	4,4′,4″,4‴-methanetetrayltetrabenzoic acid
H_4MTPA	4,4′,4″,4‴-((methanetetrayltetrakis (benzene-4,1-diyl)tetrakis(ethyne-2,1-diyl)) tetrabenzoic acid
H_4MTPB	4′,4‴,4⁗,4⁗′,4⁗″-methanetetrayltetrakis (([1,1′-biphenyl]-4-carboxylic acid))
H_4PyrDI	5,5′-(pyrimidine-2,5-diyl)diisophthalic acid
H_4QPTCA	[1,1′:4′,1″:4″,1‴:4‴,1⁗-quinquephenyl]-3,3⁗,5,5⁗-tetracarboxylic acid
H_4SFTT	4,4′,4″,4‴-(9,9′-spirobi[fluorene]-2,2′,7,7′-tetrayl)tetrabenzoic acid
H_4STBA	4,4′,4″,4‴-silanetetrayltetrabenzoic acid
H_4TBADB-18Cr6	4,4′,4″,4‴-(6,7,9,10,17,18,20,21-octahydrodibenzo[b,k][1,4,7,10,13,16] hexaoxacyclooctadecine-2,3,13,14-tetrayl) tetrabenzoic acid
H_4TBAPy	4,4′,4″,4‴-(1,8-dihydropyrene-1,3,6,8-tetrayl) tetrabenzoic acid

H_4TCBPP-H_2	4′,4‴,4⁗,4⁗′-(porphyrin-5,10,15,20-tetrayl)tetrakis(([1,1′-biphenyl]-4-carboxylic acid))
H_4TCPP-H_2	4,4′,4″,4‴-(porphyrin-5,10,15,20-tetrayl) tetrabenzoic acid
H_4TPTC	terphenyl-3,3′,5,5′-tetracarboxylaic acid
H_5PTPCA	5′-(4-carboxyphenyl)-[1,1′:3′,1″-terphenyl]-3,3″,5,5″-tetracarboxylic acid
H_6BHEHPI	1,3,5-tris[(1,3-carboxylic acid-5-(4-(ethynyl) phenyl))butadiynyl]-benzene
H_6BHEI	5,5′,5″-(benzene-1,3,5-triyltris(buta-1,3-diyne-4,1-diyl))triisophthalic acid
H_6HTTEI	5,5′,5″-(((benzene-1,3,5-triyltris(ethyne-2,1-diyl))tris(benzene-4,1-diyl))tris(ethyne-2,1-diyl))triisophthalic acid
H_6PTEI	4,4′-((5′-(4-((4-((oxo-λ^3-methyl)-λ^3-oxidaneyl) phenyl)ethynyl)phenyl)-[1,1′:3′,1″-terphenyl]-4,4″-diyl)bis(ethyne-2,1-diyl))dibenzoic acid
H_6TDCPB	4,4′,4″,4‴,4⁗,4⁗′-((nitrilotris(benzene-4,1-diyl))tris(azanetriyl))hexabenzoic acid
H_6TPBTM	5,5′,5″-((benzene-1,3,5-tricarbonyl) tris(azanediyl))triisophthalic acid
H_6TTA	5′,5‴-bis(4-carboxyphenyl)-5″-(4,4″-dicarboxy-[1,1′:3′,1″-terphenyl]-5′-yl)-[1,1′:3′,1″:3″,1‴:3‴,1⁗-quinquephenyl]-4,4⁗-dicarboxylic acid
H_6TTATP	5,5′,5″-((1,3,5-triazine-2,4,6-triyl) tris(azanediyl)triisophthalic acid
H_8BPTCD	9,9′,9″,9‴-([1,1′-biphenyl]-3,3′,5,5′-tetrayl) tetrakis(9H-carbazole-3,6-dicarboxylic acid)
H_8MTBDA	4′,4‴,4⁗,4⁗′-methanetetrayltetrakis (([1,1′-biphenyl]-3,5-dicarboxylic acid))
H_8TBCPPP-H_2	5′,5⁗,5⁗′,5⁗″-(porphyrin-5,10,15,20-tetrayl)tetrakis(([1,1′:3′,1″-terphenyl]-4,4″-dicarboxylic acid))
H_8TDPEPE	4′,4‴,4⁗,4⁗′-(ethene-1,1,2,2-tetrayl) tetrakis(([1,1′-biphenyl]-3,5-dicarboxylic acid))
HATP	2,3,6,7,10,11-hexaaminoterphenylene
HDN	hydrodenitrogenation
HEIMIM	(*E*)-2-(((2-hydroxyethyl)imino)methyl) imidazolate
HHTP	2,3,6,7,10,11-hexahydroxyterphenylene
HKUST	Hong Kong University of Science and Technology

HKUST-1	$Cu_3(BTC)_2$
HPP	1,3,4,6,7,8-hexahydro-2*H*-pyrimido [1,2-a]pyrimidine
HR-PXRD	High resolution X-ray diffraction
HSAB	hard-soft acid–base
IAST	ideal adsorbed solution theory
ICOF-1	$[(OHM)(TMB)_2]_{spiroborate}$
ICP	inductively coupled plasma
In-soc-MOF	$[In_3O(H_2O)_3]_2(ABDC)_3(NO_3)$
*i*Pr	iso-propyl
IRMOF-74-III	Mg(DOT-III)
IRMOF-74-III(CH_2NH_2)	Mg(CH_2NH_2-DOT-III)
IRMOF-74-III(CH_2NHMe)	Mg(CH_2NHMe-DOT-III)
IRMOF-993	$Zn_4O(ADC)_3$ pcu topology (theoretical)
IUPAC	International Union of Pure and Applied Chemistry
IZA	Structure Commission of the International Zeolite Association
JUC-77	In(OH)(OBA)
KAUST-7 or NbOFFIVE-1-Ni	$Ni(Pyr)_2(NbOF_5$
Keggin Type POM	$(NH_4)_3[(XO_4)Mo_{12}O_{36}])$, X = P, Si, S among others and M = Mo, W
L-Asp	L-aspartate
LD_{50}	The median lethal dose in toxicology. LD_{50} = lethal dose, 50%
LMCT	ligand-to-metal charge transfer
LNG	liquefied natural gas
LZU-1	$[(TFP)_2(PDA)_3]_{imine}$
MAF-25	$Mn_2^{2+}Cl_2$(BBTA)
MAF-25-ox	$Mn^{2+}Mn^{3+}(OH)Cl_2$(BBTA)
MAF-27	$Co_2^{2+}Cl_2$(BBTA)
MAF-27-ox	$Co^{2+}Co^{3+}(OH)Cl_2$(BBTA)
MAF-49	$[Zn(BATZ)](H_2O)_{0.5}$
MAF-X8	Zn(MPBA)
MAMS-1	Ni_8(5-BBDC)$_6(\mu_3\text{-}OH)_4$
m-BDC	isophthalic acid
mBIM	5-methyl-1*H*-benzo[*d*]imidazole
mBIM	6-methylbenzimidazolate
Me	methyl
Me_2-H_2TPDC	2′,5′-dimethyl-[1,1′:4′,1″-terphenyl]-4,4″-dicarboxylic acid
Me_4-BPDC	2,2′,6,6′-tetramethylbiphenyl-4,4′-dicarboxylic acid
Me_4-DMOF	Zn(Me_4-BDC)$(DABCO)_{0.5}$
MeAPO	metal-aluminophosphate
MeAPSO	metal-silicoaluminophosphate
MeOH	methanol

MeOHIM	2-hydroxymethylimidazolate
MIL	Materials Institute Lavoisier
MIL-100	$[M_3O(H_2O)_2L](BTC)_2/[M_3OL_3](BTC)_2$
MIL-100(Fe_BTB)	$[Fe_3O(H_2O)_2(L)](BTB)_2$
MIL-101	$[M_3OL_3](BDC)_3$
MIL-125	$Ti_8O_8(OH)_4(BDC)_6$
MIL-125(NH_2)	$Ti_8O_8(OH)_4(NH_2\text{-}BDC)_6$
MIL-53	M(OH)(BDC)
MIL-88	$Fe_3O(OH)(H_2O)_2(BDC)_3$
mIM	2-methyl-1*H*-imidazole
mmen	*N*,*N*′-dimethylethylenediamine
MMM	mixed-matrix membranes
MOF	metal-organic framework
MOF-177	$Zn_4O(BTB)_2$
MOF-180	$Zn_4O(BTE)_2$
MOF-2	$Zn(BDC)(H_2O)$
MOF-200	$Zn_4O(BBC)_2$
MOF-205	$Zn_4O(BTB)_{4/3}(NDC)$
MOF-210	$(Zn_4O)_3(BPDC)_4(BTE)_3$
MOF-325	$Cu_3(H_2O)_3[(Cu_3O)(PyC)_3(NO_3)L_2]_2$
MOF-5	$Zn_4O(BDC)_3$
MOF-520	$Al_8(OH)_8(HCOO)_4(BTB)_4$
MOF-520-BPDC	$Al_8(OH)_8\ (BTB)_4(BPDC)_2$
MOF-525	$Zr_6O_4(OH)_4(TCPP\text{-}H_2)_3$ (ftw topology)
MOF-545	$Zr_6O_4(OH)_4(TCPP\text{-}H_2)_2(H_2O)_8$ (scsq topology)
MOF-74	$M_2(DOT)$
MOF-801	$Zr_6O_4(OH)_4(fumarate)_{12}$
MOF-808	$Zr_6O_4(OH)_4(HCOO)_6(BTC)_2$
MOF-812	$Zr_6O_4(OH)_4(MTB)_3(H_2O)_2$
MOF-841	$Zr_6O_4(OH)_4(MTB)_2(HCOO)_4(H_2O)_4$
MOF-901	$Ti_6O_6(OCH_3)_6(AB)_6$
MOP	metal-organic polyhedron
MS	mass spectroscopy
MTV	multivariate
MUF	Massey University Metal–Organic Frameworks
MUF-7a	$(Zn_4O)_3(BTB)_{4/3}(BDC)_{1/2}\ (BPDC)_{1/2}$
MWC	maximum working capacity
NASA	National Aeronautics and Space Administration
nBIM	6-nitrobenzimidazolate
NBPDA	4-(*tert*-butoxycarbonylamino)-aniline
n-BuLi	*n*-butyllithium
NG	natural gas
NH_2-H_2BDC	2-aminoterephthalic acid

NH_2-H_2TPDC	2′-amino-[1,1′:4′,1″-terphenyl]-4,4″-dicarboxylic acid
nIM	2-nitroimidazolate
NLDFT	nonlinear density functional theory
NLDFT	nonlinear density functional theory
NMP	*N*-methyl-2-pyrrolidone
NMR	nuclear magnetic resonance
NOTT	Nottingham
NOTT-101	$Cu_2(H_2O)_2$(TPTC)
NOTT-103	$Cu_2(H_2O)_2$(2,6-NDI)
NOTT-109	$Cu_2(H_2O)_2$(1,4-NDI)
NU	Northwestern University
NU-100	$Cu_3(H_2O)$(HTTEI)
NU-1000	$Zr_6(\mu_3\text{-}OH/O)_8(H_2O,OH)_8(TBAPy)_2$
NU-110	$Cu_3(H_2O)$(BHEHPI)
NU-902	$Zr_6O_4(OH)_4$(TCPP-H_2)$_2(H_2O)_4(OH)_4$ (scu topology)
OAc	acetate, CH_3COO^-
OHM	octa-hydroxy functionalized macrocycle
O_h-nano-Ag	octahedral silver nanocrystal
OTf	triflate
OX	oxalate
PCN	porous coordination network
PCN-125	$[Cu_2(H_2O)_2]$(TPDC)
PCN-13	$Zn_4O(H_2O)_3(ADC)_3$
PCN-14	$Cu_2(H_2O)_2$(ADIP)
PCN-223	$Zr_6O_4(OH)_4$(TCPP-H_2)$_3$ (shp topology)
PCN225	$Zr_6O_4(OH)_4$(TCPP-H_2)$_2(H_2O)_4(OH)_4$ (sqc topology)
PCN-332	$[M_3O(H_2O)_2(L)](BTTC)_2$
PCN333	$[M_3O(H_2O)_2(L)](TATB)_2$
PCN-6	$Cu_3(TATB)_2$ interpenetrated
PCN-6′	$Cu_3(TATB)_2$
PCN-61	$Cu_3(H_2O)_3$(BTEI)
PCN-610	$Cu_3(H_2O)$(HTTEI)
PCN-68	$Cu_3(H_2O)_3$(PTEI)
PCN-700	$Zr_6O_4(OH)_4(Me_2\text{-}BPDC)_4(OH)_4(H_2O)_4$
PCN-700	$Zr_6O_4(OH)_8(H_2O)_4(Me_2\text{-}BPDC)_{8/2}$
PCN-701	$Zr_6O_4(OH)_6(H_2O)_2(Me_2\text{-}BPDC)_{8/2}(BDC)_{2/2}$
PCN-702	$Zr_6O_4(OH)_6(H_2O)_2(Me_2\text{-}BPDC)_{8/2}(Me_2\text{-}TPDC)_{1/2}$
PCN-703	$Zr_6O_4(OH)_6(H_2O)_2(Me_2\text{-}BPDC)_{8/2}(BDC)_{2/2}(Me_2\text{-}TPDC)_{1/2}$
PCN-777	$Zr_6O_4(OH)_4(HCOO)_6(TATB)_2$
PCN-9	$Cu_3(HTB)_2$ interpenetrated
PCN-9′	$Cu_3(HTB)_2$
PDA	1,4-phenylenediamine

PDA-$(OH)_2$	2,5-dihydroxy-1,4-phenylenediamine
PDAN	2,2′-(1,4-phenylene)diacetonitrile
PDB	0,13,16,19,22,25-octaoxa-2(2,9)-phenanthrolina-1,3(1,4)-dibenzenacyclohexacosaphane
PDH	1,4-dicarbonyl-phenyl-dihydrazide
PET	polyethyleneterephthalate
PIC	γ-picoline
PI-COF-1	$[(TAPA)_2(PMDA)_3]_{imide}$
PI-COF-2	$[(TAPB)_2(PMDA)_3]_{imide}$
PI-COF-3	$[(TABPB)_2(PMDA)_3]_{imide}$
PI-COF-4	$[(TAA)(PMDA)_2]_{imide}$
PI-COF-5	$[(TAM)(PMDA)_2]_{imide}$
PMDA	pyromellitic dianhydride
PMOF-1	$Cu_3(H_2O)(TPBTM)$
POM	polyoxometallate
PSA	pressure swing adsorption
PSE	post-synthetic linker exchange
PSM	post-synthetic modification
PT	*tert*-butyl pyrenetetraone
PTA	phosphotungstic acid
PTO	2,7-di-*tert*-butyl-pyrene-4,5,9,10-tetraone
Pur	purine
PVP	polyvinylpyrolidone
PX	*p*-xylene
PXRD	powder X-ray diffraction
Py	pyridine
PyC	4-pyrazolecarboxylic acid
Pyr	pyrazine
PyTA	4,4′,4″,4‴(Pyrene-1,3,6,8-tetrayl)tetraaniline
QCM	quartz crystal microbalance
Q_{st}	isoteric heat of adsorption
RCSR	reticular Chemistry Structure Resource
RED	3D rotation electron diffraction
RH	relative humidity
rho Z-MOF	$In(HIMDC)_2(HPP)$ with **rho** topology
rht-MOF-1	$[Cu_3(TZI)_2(H_2O)_2]_{12}[Cu_3O(OH)(H_2O)_2]_8$
RON	research octane number
ROX	roxorsone
RPM3-Zn	$Zn_2(BPDC)_2(BPEE)$
SALE	solvent assisted linker exchange
SALEM-1	$Cd(mIM)_2$
SALI	solvent assisted ligand incorporation
SAPO	silicoaluminophosphate
SBU	secondary building unit
SDA	structure directing agent
SEM	scanning electron microscope

SIFSIX-2-Cu	$Cu(DPA)_2(SiF_6)$
SIFSIX-2-Cu-i	$Cu(DPA)_2(SiF_6)$ interpenetrated
SIFSIX-3-Ni	$Ni(Pyr)_2(SiF_6)$
SLG	single layer graphene
SLI	sequential linker installation
S-MOF-808	$Zr_6O_5(OH)_3(BTC)_2(SO_4)_{2.5}(H_2O)_{2.5}$
sod Z-MOF	$In(HIMDC)_2(HIM)$ with **sod** topology
sp^2C-COF	$[(TFPPy)(PDAN)_2]_{acrylonitrile}$
SQ	squaric acid
ST-1	$(Zn_4O)_3(TATAB)_4(BDC)_3$
ST-2	$(Zn_4O)_3(TATAB)_4(NDC)_3$
ST-3	$(Zn_4O)_3(TATAB)_4(BPDC)_2(BDC)$
ST-4	$(Zn_4O)_5(TATAB)_4(BPDC)_6$
STM	scanning tunneling microscopy
SUC	succinonitrile
TAA	1,3,5,7-tetraaminoadamantane
TABPB	1,3,5-tris[4-amino(1,1biphenyl-4-yl)]benzene
TAM	tetra-(4-aminophenyl)methane
TAPA	tris(4-aminophenyl)amine
TAPB	1,3,5-tris(4-aminophenyl)benzene
TAPB	1,3,5-tris(4-aminophenyl)benzene
TBPM	tetra(4-dihydroxyborylphenyl)methane
TBPS	tetra(4-dihydroxyborylphenyl)silane
TBPy	5,5′-bis(2-(5′-methyl-[2,2′-bipyridin]-5-yl)ethyl)-2,2′-bipyridine
TBU	tertiary building unit
TCA	(1,1′,3′,1″-Terphenyl)-3,3″,5,5″-tetracarbaldehyde
TCAT	4-(*tert*-butyl)benzene-1,2-diol
TCP	4,4′,4″,4‴-(porphyrin-5,10,15,20-tetrayl) tetrabenzonitrile
TCTPM	4,4′,4″,4‴-tetracyanotetraphenylmethane
TEM	transmission electron microscope
TEM	transmission electron microscopy
TEMPO	4-azido-2,2,6,6-tetramethyl-1-piperidinyloxy
TEOA	triethanolamine
TFA	trifluoro-acetic acid
TFB	1,3,5-triformyl-benzene
TFP	1,3,5-tris-(4-formylphenyl)-benzene
TFP	triformylphloroglucinol
TFPPy	4,4′,4″,4‴-(pyrene-1,3,6,8-tetrayl) tetrabenzaldehyde
TGA	thermogravimetric analysis
THF	tetrahydrofuran
TMB	trismethoxy borate
TMTPDC	2′,3′,5′,6′-tertramethylterphenyl-4,4″-dicarboxylic acid

TPa-1	$[(TFP)_2(PDA)_3]_{\beta\text{-ketoenamine}}$
TPP	5,10,15,20-tetra(pyridin-4-yl)porphyrin
TSA	temperature swing adsorption
TTH	(9s,10s)-13,16-diethyl-9,10-dihydro-9, 10-[1,2]benzenoanthracene-2,3,6,7-tetraol
UiO	University of Oslo
UiO-66	$Zr_6O_4(OH)_4(BDC)_{12}$
UiO-67	$Zr_6O_4(OH)_4(BPDC)_{12}$
UiO-68	$Zr_6O_4(OH)_4(TPDC)_{12}$
UMCM	University of Michigan Crystalline Material
UMCM-1	$Zn_4O(BDC)(BTB)_{4/3}$
UMCM-1(NH_2)	$Zn_4O(BDC)(BTB)_{4/3}$
UMCM-10	$Zn_4O(BDC)_{0.75}(Me_4\text{-}BPDC)_{0.75}(TCA)$
UMCM-11	$Zn_4O(BDC)_{0.75}(EDDC)_{0.75}(TCA)$
UMCM-12	$Zn_4O(BDC)_{0.75}(MTMTPDC)_{0.75}(TCA)$
UMCM-150	$Cu_3(BHTC)_2(H_2O)_3$
UMCM-2	$Zn_4O(T^2DC)(BTB)_{4/3}$
UMCM-309a	$Zr_6O_4(OH)_4(BTB)_6(OH)_6(H_2O)_6$
UMCM-4	$Zn_4O(BDC)_{1.5}(TCA)$
usf-Z-MOF	$In_5(HIMDC)_{10}(1,2\text{-}H_2DACH)_{2.5}$ with **med** topology
UTSA-76	$Cu_3(H_2O)_3(PyrDI)$
UV–Vis	ultraviolet–visible spectroscopy
VED	volumetric energy density
VSA	vacuum swing adsorption
XAS	X-ray absorption spectroscopy
XPS	X-ray photoelectron spectroscopy
ZABU SBU	$Zn_8O_2(AD)_4(-COO)_{12}$
ZIF	zeolitic imidazolate framework
ZIF-20	$Zn(Pur)_2$
ZIF-300	$Zn(2\text{-}mIM)_{0.86}(bBIM)_{1.14}$
ZIF-301	$Zn(2\text{-}mIM)_{0.94}(cBIM)_{1.06}$
ZIF302	$Zn(2\text{-}mIM)_{0.67}(mBIM)_{1.33}$
ZIF-376	$Zn(nbIM)_{0.25}(mIM)_{0.25}(IM)_{1.5}$
ZIF-412	$Zn(BIM)_{1.13}(nIM)_{0.62}(IM)_{0.25}$
ZIF-414	$Zn(nbIM)_{0.91}(mIM)_{0.62}(IM)_{0.47}$
ZIF-486	$Zn(nbIM)_{0.20}(mIM)_{0.65}(IM)_{1.15}$
ZIF-68	Zn(BIM)(nIM)
ZIF-7	$Zn(BIM)_2$
ZIF-8	$Zn(mIM)_2$
ZIF-90	$Zn(aIM)_2$
ZIF-91	$Zn(MeOHIM,aIM)_2$
ZIF-92	$Zn(HEIMIM,aIM)_2$
Z-MOF	metal-organic framework with zeolitic topology

Part I

Metal-Organic Frameworks

1

Emergence of Metal-Organic Frameworks

1.1 Introduction

Reticular chemistry[1] is the study of linking discrete chemical entities (molecules and clusters) by strong bonds to make extended structures such as metal-organic frameworks (MOFs). In MOFs, polynuclear metal clusters are joined together by organic linkers to make crystalline porous frameworks. MOFs combine the synthetic control exercised in making organic molecules with the vast geometric and compositional variations possible by using inorganic units. The reticular chemistry of MOFs has combined two fields of chemistry that have been practiced and taught separately, into one. Accordingly, the synthesis of MOFs requires the well-honed skills of both organic and inorganic chemists to make extended solids with precisely designed structures and properties. These are imparted by the constituents yet go beyond what would be possible by the individual molecular building units. One such property is the open space encompassed by the framework into which molecules can be introduced and transformed in a manner not possible otherwise. Given the potential of reticular synthesis and the place it is beginning to occupy in the larger context of chemistry, it is instructive to provide a historical perspective on how this new field has emerged. Since MOFs were the first class of crystalline solids to be developed in the realm of reticular chemistry, their history figures prominently in its initial development.

1.2 Early Examples of Coordination Solids

The field of synthetic metal-organic chemistry as it is practiced today has emerged from coordination chemistry. Early examples of transition metal complexes were discovered by serendipity centuries ago and at that time only little was known about their structure and composition. The first reported example of a synthetic coordination compound can be traced back to the discovery of the pigment "Prussian blue" in Berlin, Germany, in the beginning of the eighteenth century [1]. The story of this finding is captured in a book by Georg E. Stahl [2]. According to him, the discovery of Prussian blue took place

1 The term "reticular" is derived from Latin "*rēticulum*" meaning "*having the form of a net*" or "netlike."

Introduction to Reticular Chemistry: Metal-Organic Frameworks and Covalent Organic Frameworks,
First Edition. Omar M. Yaghi, Markus J. Kalmutzki, and Christian S. Diercks.

Companion website: www.wiley.com/go/yaghi/reticular

in the laboratories of Johann K. Dippel who was preparing a so-called "animal oil" by distillation of animal materials. This was then repeatedly distilled from potash (K_2CO_3) to remove undesired impurities. This procedure promotes the decomposition of organic components to form cyanide, which subsequently reacts with residual iron from the animal blood to form hexacyanoferrate ions $[M_2Fe(CN)_6]$ ($M = Na^+, K^+$), which stays behind as an impurity in the potash. At that time, a color maker named Johann J. Diesbach worked in Dippel's laboratory synthesizing "Florentine lake," an organic red pigment based on cochineal red. Usually, he accomplished this by precipitation of an extract of cochineal with potash and the addition of alum $[KAl(SO_4)_2 \cdot 12H_2O]$ and iron sulfate ($FeSO_4$) to enhance both the color and the processing of the resulting pigment. At one point, Diesbach had run out of potash so he borrowed some of the potash that had been used in the production of Dippel's animal oil. To his surprise, upon addition of this contaminated potash he observed an unexpected rich blue precipitate, later termed Prussian blue, $Fe_4^{3+}[Fe^{2+}(CN)_6]_3 \cdot H_2O$.

Owing to their intense colors, a variety of coordination compounds have had widespread practical use throughout history as pigments (e.g. Prussian blue) and dyes (e.g. alizarin) without knowledge of their chemical composition or structure [1c, 3]. As illustrated with this representative example, the serendipitous discoveries of coordination compounds at that time severely limited the number of accessible materials and hence conclusions about their behavior were exclusively based on phenomenological observations.

1.3 Werner Complexes

The conceptual foundation of coordination chemistry was laid by the Swiss chemist Alfred Werner, who was ultimately awarded the Nobel Prize in chemistry in 1913 for his efforts [4]. When he started his career in 1890 he tried to elucidate and conceptualize the spatial arrangement of atoms in coordination complexes [5]. In 1857, F. August Kekulé proposed the model of constant valence, which was based on the general assumption that every element only exists in one valence and therefore only has one fixed coordination number [6]. Chemical formulae were consequently given using the dot notation, as in $CoCl_3 \cdot 6NH_3$, which gave a correct description of the chemical composition but, as Werner later determined, did not represent the actual molecular structure (Figure 1.1).

A key observation that led to this conclusion was that addition of hydrochloric acid to a solution of $CoCl_3 \cdot 6NH_3$ did not result in the quantitative liberation of all six ammonia molecules per complex. The fact that some ammonia was

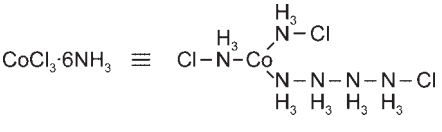

Figure 1.1 Chemical structure of $CoCl_3 \cdot 6NH_3$ based on the theory of constant valence. According to this theory cobalt has a valence of three and therefore has three ligands attached (trigonal arrangement) with the remaining ligands forming chains.

not released led Werner to deduce that it must be bound tightly to the central cobalt atom. In contrast, upon addition of aqueous silver nitrate, all the chloride ions were precipitated as silver chloride. Furthermore, in experiments conducted on a series of compounds of general formula $CoCl_3 \cdot n NH_3$ (n = 1–6) containing various amounts of ammonia, the amount of silver chloride formed by addition of silver nitrate was shown to be directly proportional to the number of ammonia molecules bound to the Co^{3+} center (Figure 1.2)[2] [7c]. Werner carried out conductivity measurements on solutions containing these different complexes, where he observed a trend in conductivity that could be directly correlated to the number of free chloride ions [8]. Based on these findings, Werner concluded that an attractive force must exert uniformly from the central metal ion toward all parts of its surface and that six ligands arrange around this center of attraction in order to minimize the interactions between themselves but maximize their interactions with the metal ion. According to this new concept the aforementioned complexes were denoted as $[Co(NH_3)_6]Cl_3$, $[Co(NH_3)_5Cl]Cl_2$, and $[Co(NH_3)_4Cl_2]Cl$, illustrating that they are in fact built from six ligands surrounding one central Co^{3+} ion.

The coordination number 6 found for this complex can adopt three different geometries: hexagonal planar, trigonal-prismatic, and octahedral. These geometries can be distinguished by the number of their possible isomers. In order to determine the geometry of $CoCl_3 \cdot n NH_3$ complexes (i.e. which one of these conformations is in fact favored) Werner conducted detailed studies on $[Co(NH_3)_4Cl_2]Cl$. For this complex, a hexagonal planar or trigonal prismatic coordination affords three different stereoisomers, whereas the octahedral coordination can only result in two such isomers (Figure 1.3). Werner verified

$$CoCl_3 \cdot 6NH_3 \xrightarrow{Ag(NO_3)} Co(NO_3)_3 \cdot NH_3 + 3AgCl \Longrightarrow [Co(NH_3)_6]Cl_3$$

$$CoCl_3 \cdot 5NH_3 \xrightarrow{Ag(NO_3)} Co(NO_3)_2Cl \cdot NH_3 + 2AgCl \Longrightarrow [Co(NH_3)_4Cl]Cl_2$$

$$CoCl_3 \cdot 4NH_3 \xrightarrow{Ag(NO_3)} Co(NO_3)Cl_2 \cdot NH_3 + 1AgCl \Longrightarrow [Co(NH_3)_5Cl_2]Cl$$

Figure 1.2 Precipitation of silver(I) chloride by addition of silver(I) nitrate to solutions of different ionization isomers of $CoCl_3 \cdot n NH_3$. The amount of silver(I) chloride precipitated was found to be different for each isomer. The chemical formulae shown on the right indicate a coordination number of 6 for the Co^{3+} center.

Figure 1.3 Possible isomers for the octahedral complex of formula $Co(NH_3)_4Cl_2$. The violet *cis*-isomer ("violeo" complex) is shown on the left, the green *trans*-isomer ("praseo" complex) is shown on the right. The two isomers can be distinguished by their vivid red and green colors, respectively. Color code: Co, blue; N, green; Cl, pink; H, light gray.

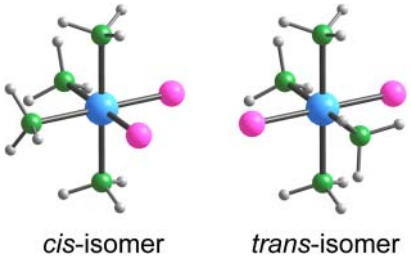

2 These findings could also be explained by the chain theory developed by Christian Blomstrand, which was later further developed by Sophus Jørgensen [7].

the latter by isolating two, not three, isomers. This work laid the foundation for the subsequent development of coordination chemistry [9].

1.4 Hofmann Clathrates

The newly gained insight into the precise molecular structure provided by Werner's work served as an inspiration to extend the practice of coordination chemistry from the molecular (0D) regime into higher dimensions, especially 2D and 3D extended structures. An early example of a coordination compound with an extended 2D structure was published by Karl A. Hofmann in 1897 [10]. Slow diffusion of C_6H_6 into an NH_3 solution of $Ni(CN)_2$ yielded a crystalline material of the general formula $[Ni(CN)_2(L)](C_6H_6)$ (L = NH_3), commonly referred to as Hofmann clathrate (Figure 1.4).[3] This compound was first speculated to be a molecular solid composed of $Ni(CN)_3(\eta^6\text{-}C_6H_6)$ molecules, but when its crystal structure was solved by single crystal X-ray diffraction, this material was found to be an extended coordination compound, built from 2D layers of alternating octahedral and square planar Ni^{2+} ions linked by CN^- ions [12]. Terminal ammonia ligands on the octahedral nickel centers pointing toward adjacent layers facilitate the formation of cavities, rendering the compound capable of encapsulating benzene as guests. These guest molecules are, as in many cases, solvent molecules trapped during the synthesis of the material that function as templates and hence play an important role in the

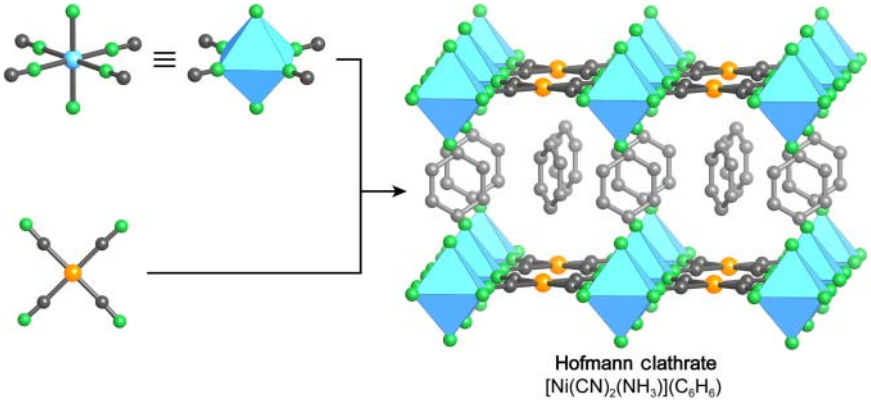

Figure 1.4 Representation of the crystal structure of the original Hofmann clathrate as determined by Herbert M. Powell and coworkers in 1952. Octahedral and square planar nickel moieties are linked by CN^- ions into stacked layers of composition $Ni(CN)_2(NH_3)$ that are separated by benzene guests. The two different coordination geometries for Ni^{2+} (d^8) can be explained by the strength of the ligand field. While strong ligands (−NH_3 and −NC) result in an octahedral splitting, a square planar splitting is more favorable for weaker ligands (−CN). All hydrogen atoms are omitted for clarity. Color code: Ni, blue and orange spheres; C, gray; N, green; benzene guest, light gray.

3 The term clathrate was first coined by Herbert M. Powell [11].

formation of the clathrate material. Structural collapse of Hofmann clathrates and related materials upon removal of the guest molecules from the structures is commonly observed.

The structural elucidation of this material sparked an interest in extended coordination compounds and consequently a variety of Hofmann clathrates have been reported. Iwamoto et al. focused on a more systematic approach for the synthesis of Hofmann-type compounds and discovered that in general this type of material is built from two different units, namely $[M_a{}^{2+}(CN)_4]^{2-}$ and $[M_b{}^{2+}(NH_3)_2]^{2+}$ (where a and b indicate different divalent metals such as Cd^{2+} or Ni^{2+}) and that the terminal ammonium ligands can be replaced by alkylamines [13]. They employed precursors of these complex ions in a reaction mixture involving neutral aromatic solvents to build structures of the general formula $[M_a(NH_3)_2M_b(CN)_4]G$ (G = benzene, aniline, pyrrole, or thiophene guest molecules) following Eq. (1.1).

$$[Ma^{2+}(CN)_4]2^- + [M_b^{2+}(NH_3)_2]^{2+} \xrightarrow{G} [M_a(NH_3)_2M_b(CN)_4] \tag{1.1}$$

After the successful substitution of the ammonia ligands by alkylamines, the next logical step was to employ bifunctional amino-linkers to connect adjacent layers (Figure 1.5) [14]. Iwamoto and coworkers demonstrated that the terminal ammonia ligands can be replaced with α,ω-diaminoalkanes that link adjacent layers and thereby create space for encapsulation of guests. The length of the organic spacer can be systematically varied to allow for size-selective inclusion of guest molecules [15].

The introduction of organic linkers between adjacent layers facilitates the adjustment of the interlayer distance and thus has a strong impact on the properties of the extended coordination compound. To increase the control

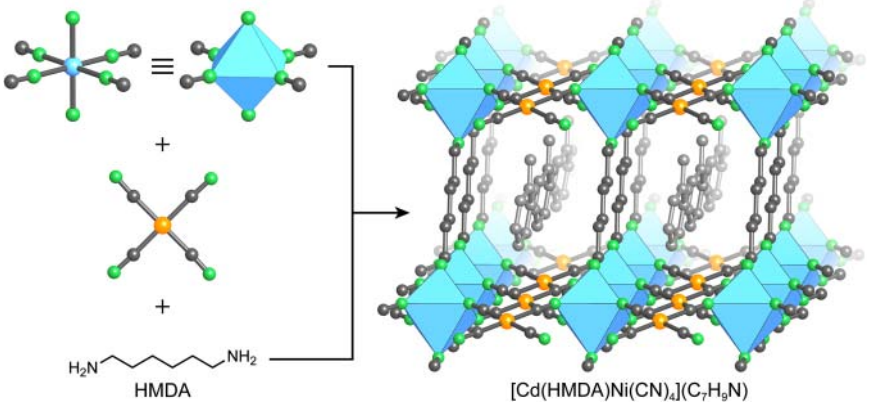

Figure 1.5 Single crystal X-ray structure of a modified Hofmann clathrate. The 2D layers of the Hofmann clathrate are linked by an α,ω-diaminoalkane (HMDA = hexametylene-1,6-diamine) into a 3D extended structure of the chemical formula $[Cd(HMDA)Ni(CN)_4](C_7H_9N)$. Disordered *o*-toluidine (C_7H_9N) guest molecules occupy the space between adjacent layers. All hydrogen atoms are omitted for clarity. Color code: Cd, blue; Ni, orange; C, gray; N, green; guest molecules, light gray.

that can be exercised over the metrics of extended structures, the next logical progression was to link metal ions entirely through organic linkers to form what have come to be known as coordination networks (also referred to as coordination polymers, although we prefer the use of the term networks as such compounds are crystalline extended structures).

1.5 Coordination Networks

The first members of this new class of materials were reported by Saito and coworkers who made use of the well-established chemistry of Cu^+ ions and linked them through bis(alkylnitrilo) units of different lengths to yield a series of crystalline materials with structures of varying dimensionality [16]. While the use of a short linker such as succinonitrile (SUC) results in a 1D structure, slightly longer linkers favor the formation of layers, as was shown for glutaronitrile (GLU), and further elongation leads to the formation of an interpenetrated 3D structure, as in the example of adiponitrile (ADI). The key compound in this series is $[Cu(ADI)_2](NO_3)$, which adopts a 3D structure based on the diamond net (**dia**) (Figure 1.6). The "open" architecture of this structure, owing to the length of the organic linker, leads to sixfold interpenetration, leaving enough space for the nitrate ions balancing the charge on the cationic framework.

The topological classification of $[Cu(ADI)_2](NO_3)$ is based on the geometric principles of crystal chemistry established by Alexander F. Wells, who developed a system to simplify crystal structures by describing them in terms of nets constructed from nodes and links [17].

Since this concept is frequently used to describe extended structures, especially those of MOFs, it is instructive to briefly illustrate the basics underlying this concept. Here, topology refers to a simplified representation of a crystal structure considering only the connectivity and not the chemical information or metrics of its constituents. It is invariant to bending, stretching, and collapsing, but not to the making and breaking of connections (see Chapter 18). This principle is illustrated by a fisherman's net representing a square grid similar to that of $[Cu(ADI)_2](NO_3)$ (Figure 1.6). The net retains its square grid structure whether it is folded or distorted, but loses it if one or more threads are cut in half. This principle is useful in simplifying and classifying the crystal structures of solids [18]. The nomenclature for net topologies uses three letter codes (small bolded letters) that are compiled in the reticular chemistry structure resource (RCSR) database. These names may be assigned arbitrarily but often they are related to the names of naturally occurring minerals of that specific topology (e.g. diamond, **dia**; quartz, **qtz**). The topology of the net underlying a crystal structure is derived by deconstructing it into vertices and edges (nodes and links). These are distinguished based on their number of points of extension: the number of connections to other building units within the structure. An edge has two points of extension, such as the ditopic linker adiponitrile (Figure 1.6), and a vertex is defined as a building unit with three or more points of extension, such as a metal ion with coordination number 4 or a cluster of atoms making 4 connections. These two definitions will enable us to simplify any given crystal

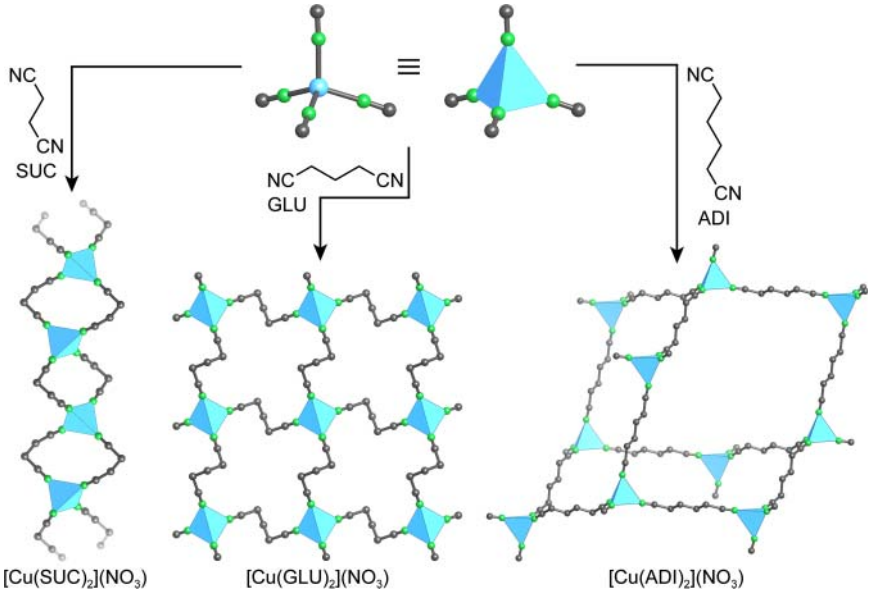

Figure 1.6 Structures of a series of bis(alkylnitrilo) linked Cu^{+} coordination networks. Short linkers such as succinonitrile (SUC) yield 1D chains of the kind shown on the left. 2D layers (one is shown) are obtained from longer glutaronitile (GLU) linkers (center), and a 3D network with **dia** topology is formed with adiponitrile (ADI) linkers (right). All hydrogen atoms are omitted and only one framework of the sixfold interpenetrated framework in the **dia** structure of $[Cu(ADI)_2](NO_3)$ is shown for clarity. Color code: Ni, blue; C, gray; N, green.

structure to a net of vertices that are linked by edges. We exercise this for the structure of $[Cu(ADI)_2](NO_3)$ with **dia** topology. Figure 1.7a shows a fragment of the $[Cu(ADI)_2](NO_3)$ structure [16c]. ADI units are 2-connected linkers while the copper atoms are 4-connected nodes as shown in Figure 1.7b in the simplified net. An even clearer representation can be achieved when adding the corresponding polyhedra or vertex figures to give the augmented net **dia-a** (Figure 1.7c). Linking metal centers through organic struts leads to the formation of frameworks encompassing open space. Within such structures this open space is sometimes filled with additional frameworks that are identical in both composition and topology. These are mechanically entangled rather than chemically linked, a phenomenon referred to as interpenetration [18]. A more detailed discussion on the topic of topology can be found in Chapter 18.

In an attempt to synthesize a radical anion salt of 2,5-dimethyl-*N*,*N*-dicyanoquinonediimine, Siegfried F. Hünig and coworkers prepared another coordination network of **dia** topology [19]. Despite the fact that its crystal structure was not discussed in detail, Akiko Kobayashi and coworkers synthesized isostructural forms using functionalized linkers bearing methoxy-, chloro-, and bromo-substituents, which have the same sevenfold interpenetrated structure [20]. Adding functionality onto the backbone of such networks, without changing the overall metrics and underlying topology, brought the molecular precision of organic chemistry into the realm of extended solids.

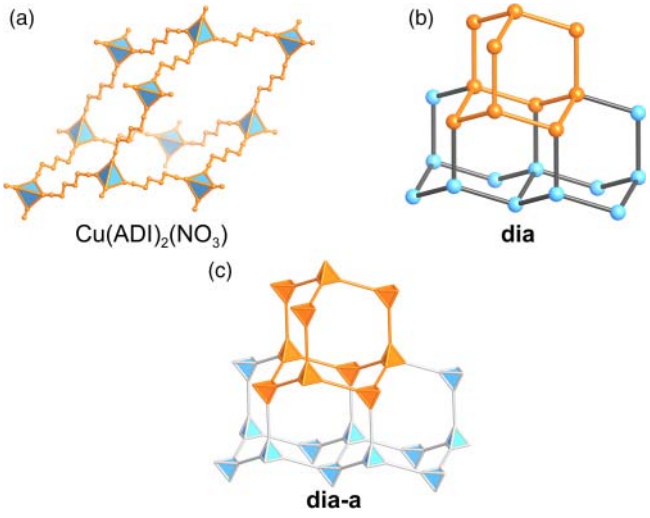

Figure 1.7 (a) Simplification of the crystal structure of $[Cu(ADI)_2](NO_3)$ adopting a diamond-like structure. (b) Representation of building units with two points of extension as edges and building units with four points of extensions as nodes yields the underlying **dia** topology. (c) Representing the vertices as their corresponding vertex figures (polyhedra) yields the augmented **dia-a** net in its highest symmetry embedding. Tetrahedral nodes are shown in blue, edges in gray. One adamantane cage is shown in (a) and highlighted in orange in (b) and (c).

The immense diversity of theoretically accessible coordination network structures made in a manner akin to the methods reported by Saito et al. inevitably led to the necessity of deploying generally applicable design principles for this class of materials. Such principles were already well developed in the field of crystal engineering, where chemists seek to understand weak interactions (C—H· · ·A, hydrogen bonds, halogen bonds, π-interactions, and van der Waals forces) between individual molecules in molecular solids in order to engineer their arrangement within the crystal [21]. Since coordination networks are also held together by rather weak non-covalent interactions (Metal–N–donor interactions), the deliberate design of coordination networks is often considered to fall under the rubric of crystal engineering [22]. In this context, Richard Robson and Bernard Hoskins recognized that Wells principles of nodes and links as outlined earlier can be applied to predict structures that will result from linking of molecular building units of a given geometry and connectivity[4] [24]. They demonstrated that this approach facilitates the deliberate design of coordination networks with predetermined structures. For example, linking tetrahedral Cu^+ single metal nodes and 4,4′,4″,4‴-tetracyanotetraphenylmethane (TCTPM) results in a non-interpenetrated coordination network of the chemical formula

4 In this paper Hoskins and Robson also report the designed synthesis of $Zn(CN)_2$ and $Cd(CN)_2$, which previously had been synthesized and described (1941 and 1945, respectively) by Zhdanov et al. and whose ability to form clathrates was reported by Iwamoto et al. in 1988 [23].

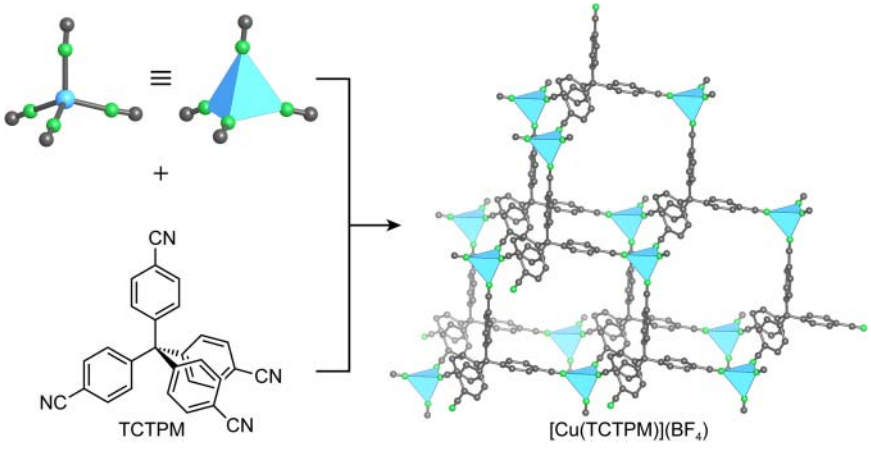

Figure 1.8 Crystal structure of the cationic coordination network $[Cu(TCTPM)](BF_4)$ (TCTPM = 4,4′,4″,4‴ tetracyanotetraphenylmethane). The network has a **dia** topology and is composed of tetrahedral Cu^+ single metal nodes and tetrahedral TCTPM linkers. All counter ions, solvent molecules, and hydrogen atoms are omitted for clarity. Color code: Cu, blue; C, gray; N, green.

$[Cu(TCTPM)](BF_4)$ and **dia** topology (Figure 1.8). The adamantane cages of this structure have an estimated pore volume of 700 $Å^3$ and are occupied by BF_4^- ions that can be exchanged with PF_6^-, as evidenced by infrared spectroscopy, while the crystallinity of the material is retained.

It was shown that the use of elongated linkers such as 1,4-dicyanobenzene, 4,4′-dipyridyl, and 2,5-dimethylpyrazine yields isostructural analogs with different degrees of interpenetration due to the different pore sizes of the resulting networks [25]. In addition to changing the metrics of the building units their general geometry and number of points of extension can be altered to yield networks of different structure types.

The combination of tetrahedral and square planar building units leads to structures based on the platinum sulfide (**pts**) net. In the first such example, Cu^+ ions were linked with $Pt(CN)_4^{2-}$ units. Here, the Cu^+ and the $Pt(CN)_4^{2-}$ units replace the tetrahedral S^{2-} and square planar Pt^{2+} ions in the structure of the PtS mineral, respectively [26]. The resulting anionic framework has the chemical formula $[CuPt(CN)_4](NMe_4)$ and the pores are filled with $(NMe_4)^+$ counter ions. Control over the metrics of the system was demonstrated by deliberate expansion of the pore size by replacing the inorganic $Pt(CN)_4^{2-}$ units with porphyrin-based square building units (Figure 1.9). Here, a cyanophenyl-functionalized porphyrin (TCP) was used as the square planar unit to give a twofold interpenetrated structure of the chemical formula $[Cu(Cu\text{-}TCP)](BF_4)$ [27]. It was then shown that interpenetration can be avoided by using a pyridyl-functionalized porphyrin linker (TPP). Linking TPP with tetrahedral Cu^+ single metal nodes gives a non-interpenetrated structure of the formula $[Cu(Cu\text{-}TPP)](BF_4)$. This finding is rationalized by the smaller internal pore space of the network constructed from TPP compared to that constructed from TCP linkers [27].

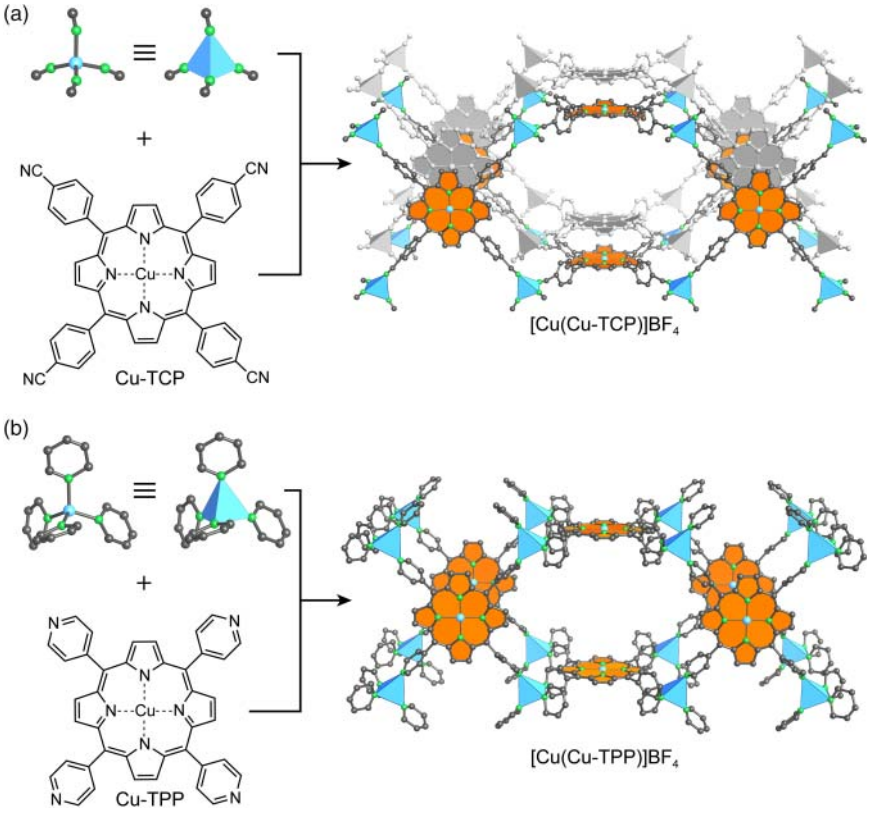

Figure 1.9 Comparison of two coordination networks built from tetrahedral Cu^{+} and square planar porphyrin-based linkers, crystallizing in the **pts** topology. (a) A twofold interpenetrated framework [Cu(Cu-TCP)](BF_4) is obtained from cyanophenyl-functionalized porphyrin (TCP) and Cu^{+} ions. (b) Replacing the terminal benzonitrile coordinating groups by pyridine groups (TPP = tetrapyridyl-functionalized porphyrin) prevents interpenetration and gives rise to the non-interpenetrated framework [Cu(Cu-TPP)](BF_4). All hydrogen atoms, counter ions, and solvent molecules are omitted for clarity. The interpenetrating net in (a) is shown in gray. Color code: Cu^{+}/Cu^{2+}, blue; C, gray; N, green; square planar porphyrin building units are highlighted as orange polygons. The crystal structure drawings are based on modified datasets where the porphyrin rings are fixed in a planar shape.

The use of geometric design principles for coordination networks and the molecular building unit approach signified an important evolution in the synthesis of extended structures. The resulting level of synthetic control was largely unknown prior to coordination networks. It is however worthy of note that at this point only a hand full of structure types was reported, most of which suffered from interpenetration and lack of accessibility of their internal pore space.

In 1990, Makoto Fujita used ethylenediamine-capped Pd^{2+} units to make a square-shaped polynuclear macrocyclic complex of composition $[(en)Pd(BIPY)(NO_3)_8]_4$ (en = ethylendiamine, BIPY = 4,4′-bipyridine) [28].

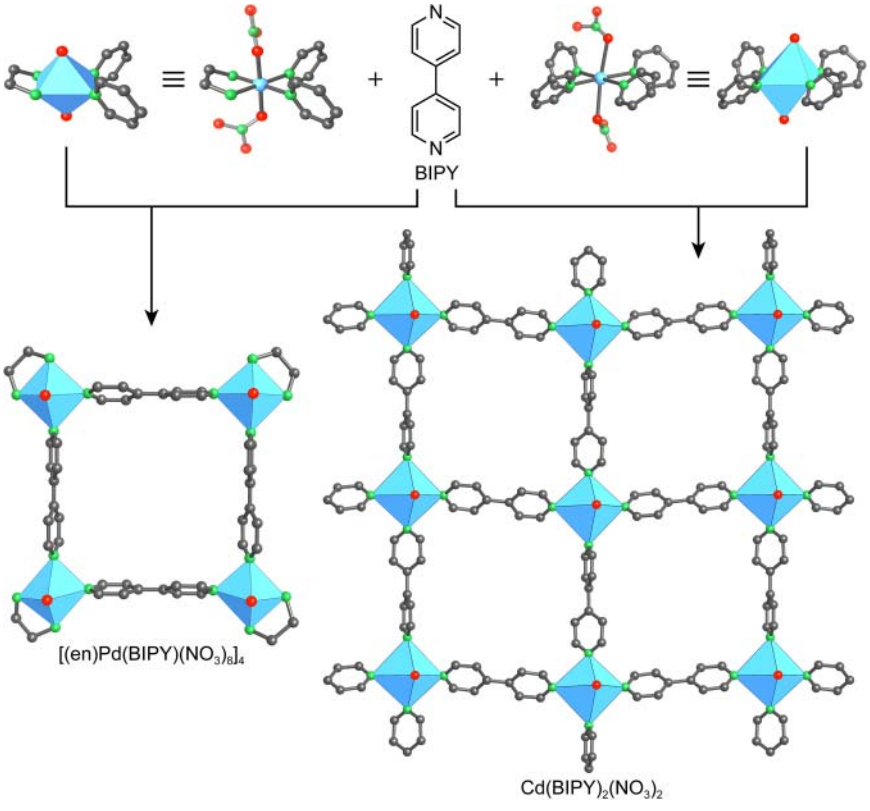

Figure 1.10 Molecular square synthesized by reacting a capped Pd^{2+} complex with BIPY. Using Cd^{2+} ions results in the formation of an extended square grid (**sql**) structure of formula $Cd(BIPY)_2(NO_3)_2$. Dichlorobenzene guest molecules reside in the square channels formed by the eclipsed stacking of the **sql** layers of the network. All guest molecules and hydrogens are omitted for clarity. Color code: Pd and Cd, blue; C, gray; N, green; O, red.

When the capped Pd^{2+} units in the synthesis of this macrocycle are replaced by uncapped Cd^{2+} ions an extended 2D square grid (**sql**) is formed (Figure 1.10) [29].

In 1995, two extended coordination networks related to $M(BIPY)_2$ were published, both of which are essential in the development of the field of MOFs. In fact, the term metal-organic framework was first coined in one of these contributions, in which Omar M. Yaghi and coworkers reported the solvothermal synthesis of $[Cu(BIPY)_{1.5}](NO_3)$ (Figure 1.11) [30]. The term metal-organic framework was originally used to describe the overall composition (metal ion and organic) and character of the structure (framework). Later on, the term MOF was more meaningfully used to describe additional structural attributes (rigidity) and properties (porosity).[5] The structure of $[Cu(BIPY)_{1.5}](NO_3)$ is built from trigonal planar Cu^+

5 Currently, the IUPAC definition of a MOF is: "A coordination network with organic ligands containing potential voids."

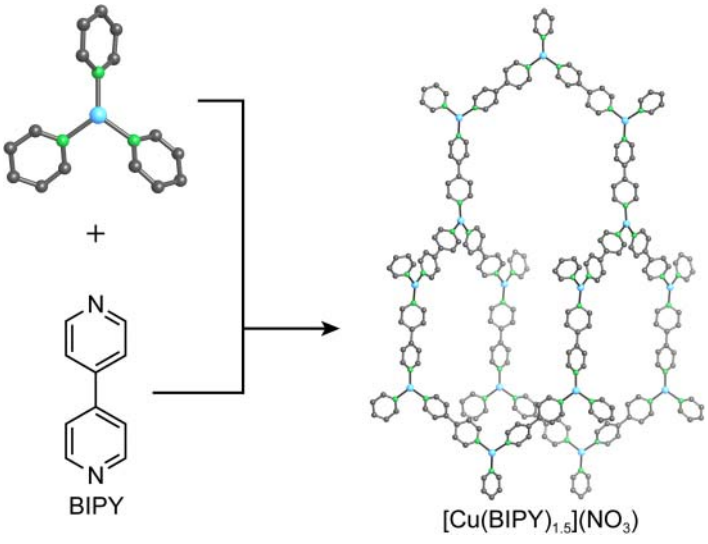

Figure 1.11 3D framework of $[Cu(BIPY)_{1.5}](NO_3)$ based on trigonal planar Cu^+ single metal nodes connected by linear BIPY linkers. The twofold interpenetrated structure has a **ths** topology. Only one cage is shown to illustrate the connectivity and orientation of the individual building units within the **ths** net. Interpenetrating frameworks, solvent molecules, counter ions residing in the channels, and all hydrogen atoms are omitted for clarity. Color code: Cu, blue; C, gray; N, green.

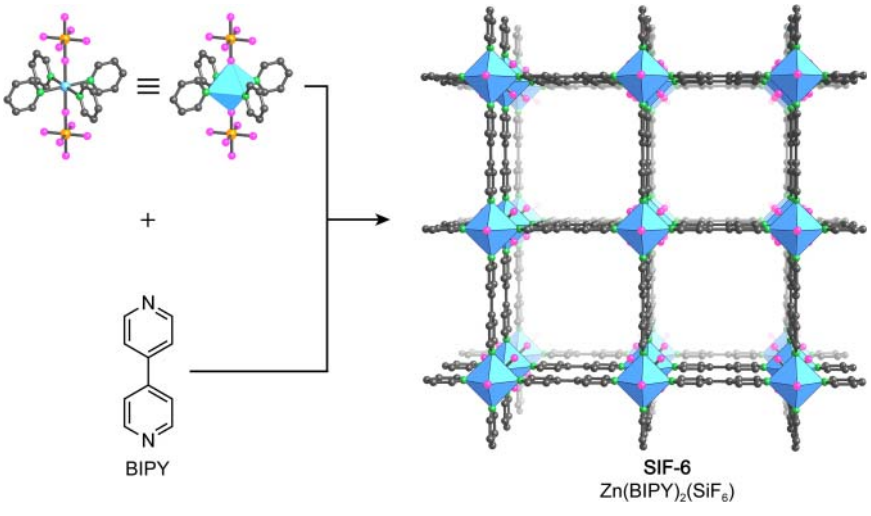

Figure 1.12 Single crystal structure of $Zn(BIPY)_2(SiF_6)$ with view along the *c*-direction. Octahedrally coordinated Zn^{2+} ions are joined by BIPY linkers to form 2D **sql** layers. These layers are pillared by SiF_6^{2-} resulting in the assembly of a charge neutral 3D **pcu** network, with channels of 8×8 Å running along the crystallographic *c*-axis. All hydrogen atoms and solvent molecules are omitted for clarity. Color code: Zn, blue; Si, orange; F, purple; C, gray; N, green.

centers connected by linear BIPY linkers to form an interpenetrated 3D network with an underlying $ThSi_2$ (**ths**) topology. The NO_3^- counter ions reside in the 8×6 Å and 4×5 Å channels of the structure and they can be readily exchanged for simple inorganic anions such as BF_4^- or SO_4^{2-} with full retention of the overall structure. The solvothermal synthesis of this material resembles the synthetic routes used in zeolite chemistry and this approach has since proven fruitful for the synthesis of many MOFs.

That same year, Michael J. Zaworotko and coworker reported a coordination network of formula $Zn(BIPY)_2SiF_6$ having a square grid of octahedral Zn^{2+} ions linked by BIPY (Figure 1.12) [31]. These layers are pillared by SiF_6^- to form a charge neutral non-interpenetrated cubic primitive structure with 8×8 Å channels running along the crystallographic *c*-direction. The potential empty space in this network represents 50% of the unit cell volume. However, the structure of $Zn(BIPY)_2SiF_6$ collapses when the guest molecules are removed from its pores.

1.6 Coordination Networks with Charged Linkers

While the aforementioned design principles can be used to construct a wide variety of coordination networks through the judicious choice of metal ions and organic linkers, the resulting materials generally suffer from inherent architectural and chemical instability. To overcome these limitations, charged chelating linkers were introduced. The use of such linkers has two important advantages: increased bond strength results in higher thermal and chemical stability and the charge on the linker can balance the charge of the cationic metal centers to circumvent the formation of ionic networks and avoid the need for counter ions filling the pores. This was first illustrated in 1995 with the synthesis of $Co(BTC)(Py)_2$ (BTC, benzene-tricarboxylate). The structure of $Co(BTC)(Py)_2$ consists of alternating stacked layers of pyridine and Co-BTC [32]. within the Co-BTC layers, each Co^{3+} ion is coordinated by three carboxylates of neighboring BTC linkers (Figure 1.13). One of the BTCs is coordinated to three metal centers in a bidentate fashion, while the other BTCs coordinate to three metal centers in a monodentate fashion. The pyridine ligands between adjacent layers provide for an interlayer distance of 7 Å. $Co(BTC)(Py)_2$ is exceptionally stable for an extended network material, decomposing only at temperatures above 350 °C. As expected, owing to the strong bonds between the metal centers and the charged BTC linkers, removal of the pyridine molecules does not lead to the collapse of the structure. The Co-BTC layers remain intact and after the pyridine guest molecules have been removed thermally, they can selectively be re-inserted between the layers, thereby regenerating the original structure as evidenced by powder X-ray diffraction.

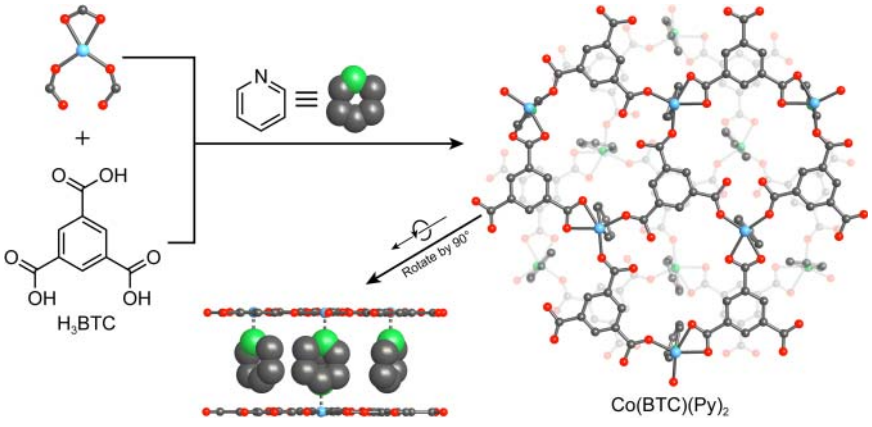

Figure 1.13 Linking Co^{3+} ions and BTC results in the formation of a layered 2D structure of formula $Co(BTC)(Py)_2$. The layers are constructed from square planar Co^{3+} and trigonal planar BTC linkers and are stacked along the crystallographic *c*-axis. The individual layers are separated by pyridine ligands coordinated to give Co^{3+} centers to given an overall octahedral coordination geometry. The pyridine guest molecules can be removed thermally and reinserted, regenerating the original structure of MOF-1 of the original structure of MOF-1. Color code: Co, blue; C, gray; N, green; O, red.

1.7 Introduction of Secondary Building Units and Permanent Porosity

To further increase the stability of metal-organic extended structures, polynuclear clusters, commonly referred to as secondary building units (SBUs), were sought as nodes to replace the single metal-ion nodes in coordination networks. The SBUs offered several advantages toward realizing more robust structures: the chelation of metal ions to make polynuclear clusters provided for rigidity and directionality while the charge on the linker led to increased bond strength and the formation of neutral frameworks. In combination, these factors were expected to contribute greatly to the overall stability of the resulting material. This concept was realized in 1998 when the synthesis and gas sorption properties of the first metal-organic framework, MOF-2 $Zn(BDC)(H_2O)$ were reported (Figure 1.14). MOF-2 has a neutral framework structure and is synthesized by slow vapor diffusion of a mixture of trimethylamine/toluene into a DMF/toluene solution of $Zn(NO_3)_2{\cdot}6H_2O$ and benzenedicarboxylic acid (H_2BDC) [33]. The layered structure of MOF-2 is built from dimeric $Zn_2(—COO)_4$ paddle wheel SBUs (rather than single metal nodes) that are linked by BDC struts to form a square grid (**sql**).

The increased stability imparted by the paddle wheel SBUs made it possible to remove all solvent molecules from the pores without collapsing the structure of MOF-2, leading to permanent microporosity as evidenced by reversible nitrogen gas adsorption at 77 K. The proof of permanent porosity in this MOF signaled a turning point in the chemistry of extended metal-organic solids and led to the use of the term MOF to emphasize their distinct stability and porosity.

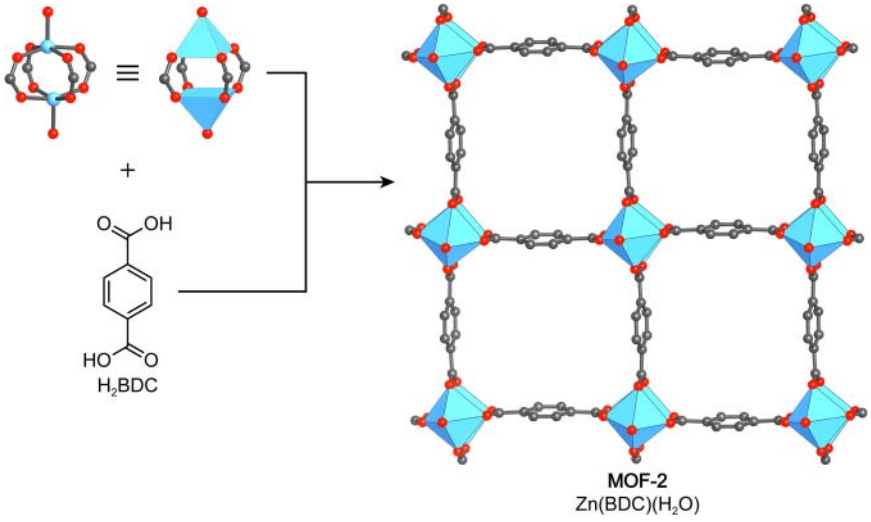

Figure 1.14 Crystal structure of MOF-2 viewed along the crystallographic *a*-axis, emphasizing the trapezoidal channels. Dinuclear Cu^{2+} paddle wheel SBUs are connected by ditopic BDC linkers to form layers of **sql** topology. The architecturally stable combination of paddle wheel SBUs and charged chelating linkers endow MOF-2 with permanent porosity. All hydrogen atoms and guest molecules are omitted for clarity. Color code: Cu, blue; C, gray; N, green; O, red.

Furthermore, this development led to extensive work on combining metals with carboxylates and other charged chelating linkers to give crystalline frameworks with SBUs as nodes. The term MOF has been overwhelmingly applied to distinguish such structures and henceforth we will adopt this terminology. The discovery of permanent porosity in MOF-2 generated interest in the further development of MOFs as it indicated that it is possible to make a wide range of 2D and 3D MOFs by combining different inorganic SBUs and organic linkers.

1.8 Extending MOF Chemistry to 3D Structures

The inorganic SBUs are polynuclear clusters in which the positions of the metal ions are locked in place by the binding groups of the linkers (in this book mainly carboxylates) as exemplified by the di-nuclear $M_2(CH_3COO)_4$ (M^{2+} = Cu, Zn) paddle wheel complex [34]. Their geometry and connectivity can be varied in order to allow for the formation of a variety of different MOF structures. These features, along with rigidity, and definitive directionality and connectivity facilitate the possibility for reticular synthesis and for the design of new, rigid, and permanently porous frameworks adopting a targeted structure. The synthetic and structural chemistry of polynuclear metal carboxylate clusters was well developed early on and many of their structures were solved soon after the discovery of X-ray diffraction by crystals [35]. As a matter of fact, the structure of the acetate capped paddle wheel clusters, as is found in the structure of MOF-2, was determined as early as 1953 [35g]. Based on the presumption that the replacement of

the capping acetate ligands with multifunctional organic molecules promotes the formation of open extended framework structures, the idea of employing other carboxylate clusters as SBUs in the formation of MOFs emerged. First attempts to extend the chemistry of MOFs into 3D involved the use of the basic zinc acetate, a tetra-nuclear carboxylate cluster coordinated by six acetates in an octahedral fashion, as an SBU [35f].

1.8.1 Targeted Synthesis of MOF-5

It was known by that time that basic zinc acetate $Zn_4O(CH_3COO)_6$ can be prepared by adding small amounts of hydrogen peroxide to a solution of a zinc salt in acetic acid [36]. This facilitates the formation of O^{2-}, which lies at the center of the resulting polynuclear cluster [37]. The knowledge of both, the synthesis route affording the molecular $Zn_4O(CH_3COO)_6$ cluster as well as that employed in the preparation of MOF-2, allowed for the deduction of a synthetic procedure targeting a 3D MOF based on octahedral $Zn_4O(—COO)_6$ SBUs and ditopic linear linkers.

One of the lessons learned from the synthesis of MOF-2 was that precise synthetic control is required in order to avoid the rapid precipitation of ill-defined amorphous powders as a result of the low reversibility of the formation of strong metal–carboxylate bonds. This is in stark contrast to structures held together by relatively weak metal–N–donor bonds (e.g. bipyridines and dinitriles) whose crystallization is relatively straightforward owing to the high reversibility and facile error correction during crystallization. In the case of MOF-2, the formation of a crystalline material was achieved by slow diffusion of a base (trimethylamine) into a solution of a mixture of the metal salt ($Zn(NO_3)_3{\cdot}6H_2O$) and the organic linker H_2BDC (benzenedicarboxylic acid). Slow deprotonation of the carboxylic acid groups of the linker slowed down the formation of MOF-2 and allowed for error correction and consequently the crystallization of MOF-2. This strategy was largely retained in the synthesis of MOF-5 and only modified by adding a small amount of hydrogen peroxide to a mixture of $Zn(NO_3)_2{\cdot}4H_2O$ and H_2BDC in analogy to the synthesis of the molecular $Zn_4O(CH_3COO)_6$ cluster, to favor the formation $Zn_4O(—COO)_6$ SBUs over the previously obtained $Zn_2(—COO)_4$ paddle wheel units.

Despite the rational approach to the synthesis of MOF-5, the bulk material that collected on the bottom of the vial turned out to be MOF-2.[6] One of the authors recalls that following this procedure, his student observed a small amount of cube-shaped crystals, having a morphology different from the main phase collecting at the bottom of the reaction vessel. These cubic crystals were floating at the meniscus of the mother liquor and adhered to the sides of the flask in the

6 Solvothermal methods to prepare MOF-5 in high yield were established in the following years where the slow diffusion of base into the reaction mixture was replaced by using DMF (dimethylformamide) or DEF (diethylformamide), which slowly decompose upon heating to release small amounts of dimethyl- or diethylamine base. It was also shown that the use of hydrogen peroxide is not needed since O^{2-} ions can be formed from trace amounts of water in the reaction mixture. Typical reaction temperatures of 80–100 °C as well as the applicability of this route to different metal salts were reported [38].

same vicinity. The comparison of the powder X-ray diffraction pattern of MOF-2 and that of these cubic crystals confirmed the presence of two structurally distinct compounds. However, when attempting to mount these cubic crystals on a single crystal X-ray diffractometer, the formation of cracks and the loss of transparency were observed, indicating the loss of mono-crystallinity and thus initially precluding their structural characterization. It proved difficult to handle this material because the crystals degraded upon loss of solvent by evaporation after they were removed from the mother liquor. Eventually, the structure of MOF-5 was determined by keeping the crystals in the mother liquor and sealing them in a capillary prior to examination by single crystal X-ray diffraction.

1.8.2 Structure of MOF-5

The synthesis, characterization, and structure of MOF-5, $[Zn_4O(BDC)_3](DMF)_x$ was reported in 1999 by Yaghi and coworkers.[7] It was shown that the structure of MOF-5 is indeed composed of octahedral $Zn_4O(—COO)_6$ SBUs, consisting of four tetrahedral ZnO_4 units sharing a common vertex, joined by ditopic BDC linkers to give a 3D framework structure of **pcu** topology (Figure 1.15). The large size (8.9 Å) and high connectivity of the SBUs in combination with the long BDC linker (6.9 Å) provide for an open porous structure with alternating interconnected pores of 15.1 and 11.0 Å in diameter, and a pore aperture of 8.0 Å.

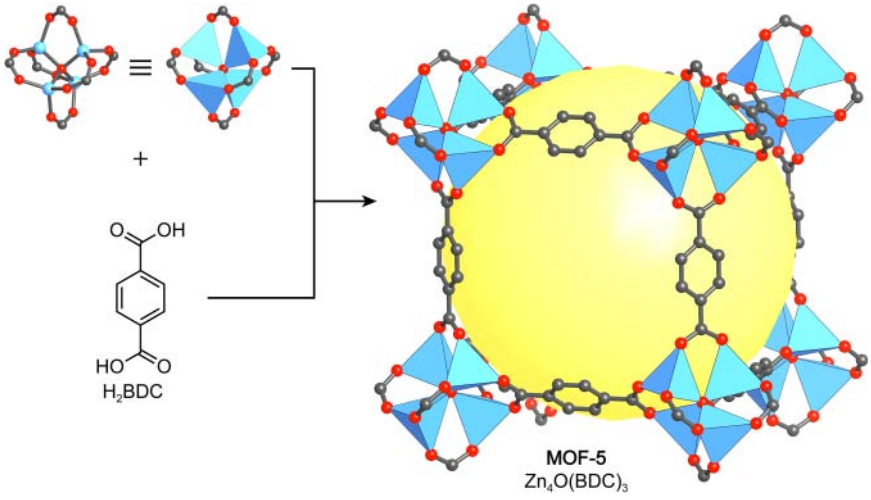

Figure 1.15 Crystal structure of MOF-5, constructed from octahedral $Zn_4O(—COO)_6$ SBUs and linear ditopic BDC linkers. The resulting primitive cubic net (**pcu**) has alternating large (15.1 Å diameter) and small (11.0 Å diameter) pores whose different size is a result of the orientation of the phenyl units of the BDC linkers with respect to the center of the pore. Only the large pore is shown for clarity. The yellow sphere indicates the largest sphere that can be placed inside the pore without coming within the van der Waals radius of any framework atom. All hydrogen atoms are omitted for clarity. Color code: Zn, blue; C, gray; O, red.

7 The name MOF-5 was chosen in analogy to the well-known zeolite ZMS-5.

These large cavities make up 61% of the unit cell volume and are filled with solvent molecules (DMF) in the as-synthesized material. One of the most striking features of the MOF-5 structure is that the pores have no walls. This provides for an unprecedented openness of the structure that allows guest molecules to move with great facility without clogging the pores. In contrast, the pores in more traditional porous solids such as zeolites have walls and diffusion can be subject to complications related to blocked pores. The structure of MOF-5 is shown in Figure 1.15 and the open space within this structure is illustrated by a yellow sphere that represents the largest sphere that can occupy the pore without penetrating the van der Waals radius of any framework atom. We will use these spheres to highlight the accessible open space within the structures of all porous frameworks discussed throughout this book.

Among the very first questions to be addressed about MOF-5 was whether the guests filling the pores could be removed without collapsing the overall structure and whether, like MOF-2, MOF-5 is stable enough to support permanent porosity. Before addressing this issue, we digress slightly to enumerate the different types of stability relevant to this and other MOFs that follow.

1.8.3 Stability of Framework Structures

Chemical stability is the ability of a given material to withstand chemical treatment without any significant change in its structure. This can be evaluated by subjecting a material to different liquid or gaseous chemicals, followed by X-ray diffraction analysis to verify that the structure of the material has not been altered or degraded.

Thermal stability is the ability of a given material to withstand thermal treatment without any significant change in its structure. This can often be assessed by thermogravimetric analysis or differential-scanning-calorimetry where, upon heating the sample, an apparent mass loss or a thermal effect (exothermic or endothermic) is recorded, indicating decomposition and changes in the structure. Additionally, X-ray diffraction studies performed on the material after or during thermal treatment can provide information on whether the structure has been retained.

Mechanical stability is the ability of a given material to withstand external forces. Methods to determine the mechanical stability of MOFs are similar to those used in materials science such as pressurization (compressibility), nano-indentation (Young's modulus) or determination of the tensile strength to name a few.

Architectural stability is the ability of a framework material to retain its structural integrity in the absence of guest molecules. It can be proven by evacuating the solvent from the pores of a MOF and subsequent confirmation of its crystal structure and porosity.

1.8.4 Activation of MOF-5

To realize the full potential of MOF-5, the challenge of removing guest molecules to yield an open framework was addressed. Initial attempts to evaporate the solvent guest molecules from the crystal caused cracking and a concomitant partial loss of porosity that were ascribed to the strong mechanical forces acting on the

framework upon solvent removal. These forces are proportional to the surface tension of the solvent in the pores and the extent of the "adhesive forces" between the guest molecules and the inner surface of the MOF. To facilitate the evacuation of the material, the highly mobile guest molecules present in the pores of the as-synthesized material were fully exchanged with chloroform ($CHCl_3$), which upon removal "puts less stress on the framework." The complete removal of all guest molecules from the pores of MOF-5 was eventually achieved by evacuation of the solvent exchanged material at 5×10^{-5} Torr and room temperature for three hours with full retention of the crystallinity of the architecturally stable framework [37]. The process of removing volatile guest molecules from the pores of MOFs is commonly referred to as "activation."

Since no change in morphology or transparency was observed upon activation of MOF-5, single crystal X-ray diffraction studies of the activated material were carried out. This is usually difficult because porous solid-state materials often lose their monocrystallinity upon removal of guest molecules. However, in this case the unit cell parameters and atomic positions determined from these measurements were shown to be almost identical to those of the as-synthesized material. In fact, the remaining electron density within the pores was significantly lower than for the as-synthesized material, providing further proof that all guest molecules had been removed and that MOF-5 is indeed permanently porous[8] [37].

1.8.5 Permanent Porosity of MOF-5

The next step in proving the permanent porosity of MOF-5 was the determination of its internal surface area. For this purpose, nitrogen adsorption experiments at 77 K (as recommended by IUPAC) were performed (Figure 1.16). These measurements allow for the determination of both pore size and surface area. The pore volume calculated from these measurements (0.54–0.61 $cm^3\ cm^{-3}$) was higher than those reported for the best performing zeolites at that time (up to 0.47 $cm^3\ cm^{-3}$) [37]. With a value of 2900 $m^2\ g^{-1}$, the Langmuir surface area reported in this contribution surpassed by far that of all zeolites, activated carbons, and other porous materials.[9] In later contributions, even higher surface areas up to 3800 $m^2\ g^{-1}$ were reported as better methods for the activation of MOFs were developed [38a].

The combination of a 6-connected $Zn_4O(—COO)_6$ cluster and charged bridging carboxylate linkers suggest that the resulting framework should exhibit high thermal stability, and indeed, neither the morphology nor the crystallinity of the fully activated MOF-5 was affected by heating the material in dry air at 300 °C for 24 hours. This was further evidenced by subsequent single crystal X-ray diffraction studies carried out on MOF-5 samples that underwent this procedure [37]. Furthermore, MOF-5 was shown to be stable at temperatures up to 400 °C under vacuum. The structural degradation of MOF-5 under atmospheric conditions can

8 A material is defined as permanently porous if it is proven to be stable upon removal of the guests from the pores without collapsing. This is measured by nitrogen gas adsorption experiments (at 77 K relative pressures between 0 and 1), the gold standard for evaluation of porosity.

9 Ulrich Müller, a research director at BASF SE, recalls his reaction when he came across this study on MOF-5 and stated: "That number was so unbelievably high, I thought it had to be a misprint." Only after having repeated the measurement himself was he convinced [39].

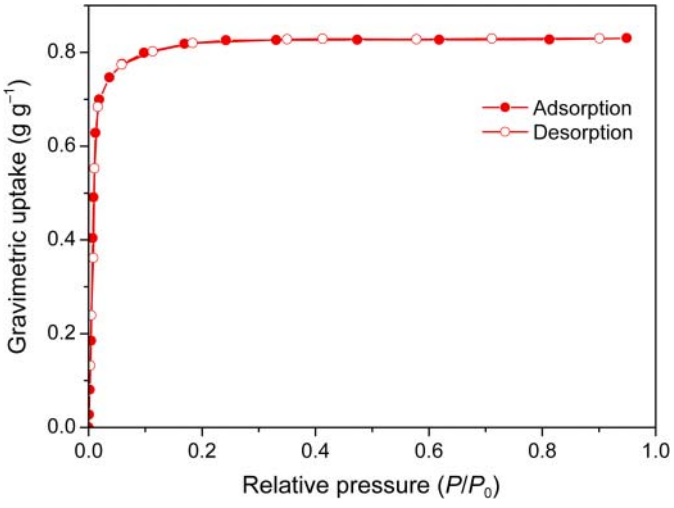

Figure 1.16 Nitrogen adsorption isotherm measured at 77 K. A pore volume of 0.54–0.61 $cm^3\ cm^{-3}$ and a Langmuir surface area of 2900 $m^2\ g^{-1}$ have been calculated from this measurement. The fact that the desorption branch perfectly traces the adsorption branch highlights the outstanding architectural and mechanical stability of MOF-5 and gives further evidence of its permanent porosity.

therefore be ascribed to humidity in the air rather than to oxygen. This is further supported by the fact that treating MOF-5 with dry solvents or dry air has no effect on its crystallinity and surface area, whereas treatment with humid air or moist solvents results in the slow decomposition of MOF-5 and the formation of a nonporous product [38a].

1.8.6 Architectural Stability of MOF-5

It is worthy of note, that when MOF-5 was first reported, there were many doubters as no one expected such an open structure, composed of largely open space, to be architecturally and thermally stable. Many expected the framework to collapse onto itself once the solvent guests are removed. To gain a deeper understanding of the key factors rendering MOF-5 architecturally stable, it is helpful to take a closer look at its structure. The cubic structure of MOF-5 (Figure 1.17a) can be deconstructed into the basic **pcu** net, that is, a framework built from single atom vertices connected by edges (Figure 1.17b). When a shear force is applied to this basic **pcu** net little resistance is expected. This however does not hold true for the actual crystal structure of MOF-5. In its crystal structure, the vertices of the basic **pcu** net are cationic zinc-oxide clusters that have an envelope[10] of truncated tetrahedral shape. These vertices are joined together by the rigid planar BDC linkers, which can be represented by a planar flat envelope (Figure 1.17c). Each set of linkers located on opposing sides of the truncated

10 The envelope representation of individual building units in carboxylate MOFs are geometrical shapes identical to those obtained when wrapping the respective building units in paper (thus envelope) while making sure, that all oxygen atoms of the carboxylate groups are touching the paper.

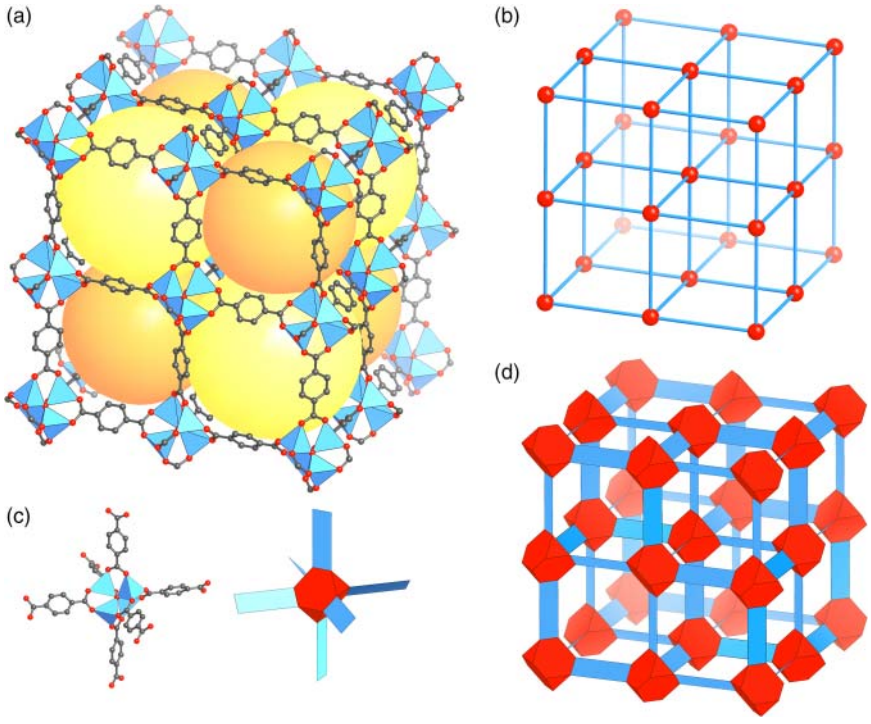

Figure 1.17 (a) Crystal structure of MOF-5, the two differently sized pores are highlighted by yellow (large pore, 15.1 Å diameter) and orange spheres (small pore, 11.0 Å), respectively. (b) Simplified representation of the basic **pcu** net of MOF-5. SBUs are replaced by single atom vertices and the BDC linkers are replaced by edges. (c) Envelope representation of the octahedral $Zn_4O(—COO)_6$ SBUs and the BDC linker as truncated tetrahedra and rectangles, respectively. (d) Envelope representation of the extended framework structure of MOF-5, highlighting its architectural stability that originates from the mutually perpendicular arrangement of BDC linkers around the SBUs. Color code: Zn, blue tetrahedra; C, gray; O, red. In the topology and envelope representation, nodes are shown in red, linkers in blue.

tetrahedron has a dihedral angle of 90°; i.e. they are rotated by 90° with respect to each other. Linking these two building units into an extended 3D framework results in an inherently rigid structure, held together by mutually perpendicular hinges (Figure 1.17d). This arrangement provides for the high architectural stability needed to allow for the activation and support of permanent porosity. The high thermal stability of MOF-5 on the other hand is attributed to the fact that the backbone of MOF-5 is composed entirely of strong bonds (Zn—O, C—O, and C—C), all of which are significantly stronger and therefore thermodynamically more stable than those in coordination networks (M–N–donor) [40].

1.9 Summary

In this chapter we have outlined the history of the development of MOFs. We showed the transition from 0D amine and nitrile-based coordination compounds

into 2D and 3D coordination networks and highlighted the key points in making robust, chemically, mechanically, and architecturally stable compounds that support permanent porosity: (i) The use of charged chelating linker and (ii) the SBU approach. In this way, the need for counter ions that reside in the pores of the framework can be avoided, and the rigidity of the building units – organic linker and SBU – renders the framework architecturally stable. We showed that different SBUs can be targeted in a rational manner, thus presenting the prospect of the designed synthesis of a vast variety of possible framework structures. In the following chapters we will consider the porosity of such frameworks in more detail.

References

1 (a) Kraft, D.A. (2012). *Wege des Wissens: Berliner Blau, 1706–1726.*; Frankfurt/Main: Gesellschaft Deutscher Chemiker/Fachgruppe Geschichte der Chemie. Bd 22. ISSN 0934-8506. https://www.gdch.de/fileadmin/downloads/Netzwerk_und_Strukturen/Fachgruppen/Geschichte_der_Chemie/Mitteilungen_Band_22/2012-22-02.pdf (b) Ball, P. (2003). *Bright Earth: Art and the Invention of Color*. Penguin. (c) Bartoll, J. (2008). Proceedings of the 9th International Conference on NDT of Art https://www.ndt.net/article/art2008/papers/029bartoll.pdf.

2 Stahl, G. (1731). Experimenta, observationes, animadversiones. *Chymicae et Physicae (Berlin)* 300: 281–283.

3 (a) Orna, M.V., Kozlowski, A.W., Baskinger, A., and Adams, T. (1994). *Coordination Chemistry: A Century of Progress*, American Chemical Society Symposium Series 565, 165–176. Washington, DC: American Chemical Society. (b) Wunderlich, C.-H. and Bergerhoff, G. (1994). Konstitution und Farbe von Alizarin- und Purpurin-Farblacken. *Chemische Berichte* 127 (7): 1185–1190.

4 (a) Kauffman, G.B. (2013). *Alfred Werner: Founder of Coordination Chemistry*. Springer Science & Business Media. (b) Constable, E.C. and Housecroft, C.E. (2013). Coordination chemistry: the scientific legacy of Alfred Werner. *Chemical Society Reviews* 42 (4): 1429–1439.

5 Werner, A. (1893). Beitrag zur konstitution anorganischer verbindungen. *Zeitschrift für Anorganische Chemie* 3 (1): 267–330.

6 (a) Kekulé, A. (1857). Ueber die sg gepaarten Verbindungen und die Theorie der mehratomigen Radicale. *European Journal of Organic Chemistry* 104 (2): 129–150. (b) Kekulé, A. (1858). Über die Constitution und die Metamorphosen der chemischen Verbindungen und über die chemische Natur des Kohlenstoffs. *European Journal of Organic Chemistry* 106 (2): 129–159.

7 (a) Blomstrand, C.W. (1869). *Chemie der Jetztzeit*. Heidelberg: C. Winter. (b) Jörgensen, S. (1894). Zur Konstitution der Kobalt-, Chrom-und Rhodiumbasen. *Zeitschrift für Anorganische und Allgemeine Chemie* 5 (1): 147–196. (c) Kauffman, G.B. (1959). Sophus Mads Jorgensen (1837–1914): a chapter in coordination chemistry history. *Journal of Chemical Education* 36 (10): 521–527.

8 Werner, A. and Miolati, A. (1894). *Zeitschrift für Physik Chem Leipzig* 14: 506–511.

9 Werner, A. (1907). Über 1.2-Dichloro-tetrammin-kobaltisalze. (Ammoniak-violeosalze). *European Journal of Inorganic Chemistry* 40 (4): 4817–4825.

10 Hofmann, K. and Küspert, F. (1897). Verbindungen von kohlenwasserstoffen mit metallsalzen. *Zeitschrift für Anorganische Chemie* 15 (1): 204–207.

11 Powell, H.M. (1948). 15. The structure of molecular compounds. Part IV. Clathrate compounds. *Journal of the Chemical Society (Resumed)* 61–73.

12 Rayner, J. and Powell, H.M. (1952). 67. Structure of molecular compounds. Part X. Crystal structure of the compound of benzene with an ammonia–nickel cyanide complex. *Journal of the Chemical Society (Resumed)* 319–328.

13 (a) Iwamoto, T., Miyoshi, T., Miyamoto, T. et al. (1967). The metal ammine cyanide aromatics clathrates. I. The preparation and stoichiometry of the diamminemetal(II) tetracyanoniccolate(II) dibenzene and sianiline. *Bulletin of the Chemical Society of Japan* 40 (5): 1174–1178. (b) Iwamoto, T., Nakano, T., Morita, M. et al. (1968). The Hofman-type clathrate: $M(NH_3)_2M'(CN)_4$. 2G. *Inorganica Chimica Acta* 2: 313–316. (c) Miyoshi, T., Iwamoto, T., and Sasaki, Y. (1972). The structure of catena-μ-ethylenediaminecadmium(II)tetracyanoniccolate(II)dibenzene clathrate: $Cd(en)Ni(CN)_4{\cdot}2C_6H_6$. *Inorganica Chimica Acta* 6: 59–64. (d) Walker, G. and Hawthorne, D. (1967). Complexes between n-alkylamines and nickel cyanide. *Transactions of the Faraday Society* 63: 166–174.

14 Nishikiori, S.-I. and Iwamoto, T. (1984). Crystal structure of Hofmann-dma-type benzene clathrate bis(dimethylamine)cadmium(II) tetracyanonickelate(II) benzene(2/1). *Chemistry Letters* 13 (3): 319–322.

15 (a) Hasegawa, T., Nishikiori, S.-I., and Iwamoto, T. (1984). *Clathrate Compounds, Molecular Inclusion Phenomena, and Cyclodextrins*, 351–357. Springer. (b) Hasegawa, T., Nishikiori, S.-I., and Iwamoto, T. (1985). Isomer selection of 1,6-diaminohexanecadmium(II) tetracyznonickelate(II) for *m*- and *p*-toluidine. Formation of 1,6-diaminohexanecadmium(II) tetracyznonickelate(II) *m*-toluidine (1/1) inclusion compound and bis(*p*-toluidine)-1,6-diaminohexanecadmium(II)tetracyznonickelate(II) complex. *Chemistry Letters* 14 (11): 1659–1662. (c) Nishikiori, S.-I., Hasegawa, T., and Iwamoto, T. (1991). The crystal structures of α,ω-diaminoalkanecadmium(II) tetracyanonickelate(II) aromatic molecule inclusion compounds. V. Toluidine clathrates of the hosts built of the diamines, 1,4-diaminobutane, 1,5-diaminonentane, and 1,8-diaminooctane. *Journal of Inclusion Phenomena and Molecular Recognition in Chemistry* 11 (2): 137–152.

16 (a) Kinoshita, Y., Matsubara, I., and Saito, Y. (1959). The crystal structure of bis(succinonitrilo)copper(I) nitrate. *Bulletin of the Chemical Society of Japan* 32 (7): 741–747. (b) Kinoshita, Y., Matsubara, I., and Saito, Y. (1959). The crystal structure of bis(glutaronitrilo)copper(I) nitrate. *Bulletin of the Chemical Society of Japan* 32 (11): 1216–1221. (c) Kinoshita, Y., Matsubara, I., Higuchi, T., and Saito, Y. (1959). The crystal structure of

bis(adiponitrilo)copper(I) nitrate. *Bulletin of the Chemical Society of Japan* 32 (11): 1221–1226.

17 Wells, A. (1954). The geometrical basis of crystal chemistry. Part 1. *Acta Crystallographica* 7 (8–9): 535–544.

18 Ockwig, N.W., Delgado-Friedrichs, O., O'Keeffe, M., and Yaghi, O.M. (2005). Reticular chemistry: occurrence and taxonomy of nets and grammar for the design of frameworks. *Accounts of Chemical Research* 38 (3): 176–182.

19 Aumüller, A., Erk, P., Klebe, G. et al. (1986). A radical anion salt of 2,5-dimethyl-*N*,*N*′-dicyanoquinonediimine with extremely high electrical conductivity. *Angewandte Chemie International Edition in English* 25 (8): 740–741.

20 Kato, R., Kobayashi, H., and Kobayashi, A. (1989). Crystal and electronic structures of conductive anion-radical salts,(2,5-R_1R_2-DCNQI)$_2$Cu (DCNQI = *N*,*N*′-dicyanoquinonediimine; R_1, R_2 = CH_3, CH_3O, Cl, Br). *Journal of the American Chemical Society* 111 (14): 5224–5232.

21 Desiraju, G.R. and Parshall, G.W. (1989). *Crystal Engineering: The Design of Organic Solids*, Materials Science Monographs, vol. 54. Elsevier.

22 Moulton, B. and Zaworotko, M.J. (2001). From molecules to crystal engineering: supramolecular isomerism and polymorphism in network solids. *Chemical Reviews* 101 (6): 1629–1658.

23 (a) Zhdanov, H. (1941). The crystalline structure of $Zn(CN)_2$. *Comptes Rendus de l'Académie des Sciences de l'URSS* 31: 352–354. (b) Shugam, E. and Zhdanov, H. (1945). The crystal structure of cyanides. II. The structure of $Cd(CN)_2$. *Acta Physicochim. URSS* 20: 247–252. (c) Takafumi, K., Shin-ichi, N., Reiko, K., and Toschitake, I. (1988). Novel clathrate compound of cadmium cyanide host with an adamantane-like cavity. Cadmium cyanide–carbon tetrachloride(1/1). *Chemistry Letters* 17 (10): 1729–1732.

24 (a) Hoskins, B.F. and Robson, R. (1989). Infinite polymeric frameworks consisting of three dimensionally linked rod-like segments. *Journal of the American Chemical Society* 111 (15): 5962–5964. (b) Hoskins, B. and Robson, R. (1990). Design and construction of a new class of scaffolding-like materials comprising infinite polymeric frameworks of 3D-linked molecular rods. A reappraisal of the zinc cyanide and cadmium cyanide structures and the synthesis and structure of the diamond-related frameworks $[N(CH_3)_4][Cu^{I}Zn^{II}(CN)_4]$ and Cu^{I}[4,4′,4″,4‴-tetracyanotetraphenylmethane]BF_4.x$C_6H_5NO_2$. *Journal of the American Chemical Society* 112 (4): 1546–1554.

25 Zaworotko, M.J. (1994). Crystal engineering of diamondoid networks. *Chemical Society Reviews* 23 (4): 283–288.

26 Gable, R.W., Hoskins, B.F., and Robson, R. (1990). Synthesis and structure of $[NMe_4][CuPt(CN)_4]$: an infinite three-dimensional framework related to PtS which generates intersecting hexagonal channels of large cross section. *Journal of the Chemical Society, Chemical Communications* (10): 762–763.

27 Abrahams, B.F., Hoskins, B.F., Michail, D.M., and Robson, R. (1994). Assembly of porphyrin building blocks into network structures with large channels. *Nature* 369 (6483): 727–729.

28 Fujita, M., Yazaki, J., and Ogura, K. (1990). Preparation of a macrocyclic polynuclear complex, $[(en)Pd(4,4'\text{-bpy})]_4(NO_3)_8$ (en = ethylenediamine, bpy = bipyridine), which recognizes an organic molecule in aqueous media. *Journal of the American Chemical Society* 112 (14): 5645–5647.

29 Fujita, M., Kwon, Y.J., Washizu, S., and Ogura, K. (1994). Preparation, clathration ability, and catalysis of a two-dimensional square network material composed of cadmium(II) and 4,4′-bipyridine. *Journal of the American Chemical Society* 116 (3): 1151–1152.

30 Yaghi, O. and Li, H. (1995). Hydrothermal synthesis of a metal-organic framework containing large rectangular channels. *Journal of the American Chemical Society* 117 (41): 10401–10402.

31 Subramanian, S. and Zaworotko, M.J. (1995). Porous solids by design: $[Zn(4,4'\text{-bpy})_2(SiF_6)]_n \cdot xDMF$, a single framework octahedral coordination polymer with large square channels. *Angewandte Chemie International Edition in English* 34 (19): 2127–2129.

32 Yaghi, O.M., Li, G., and Li, H. (1995). Selective binding and removal of guests in a microporous metal-organic framework. *Nature* 378 (6558): 703.

33 Li, H., Eddaoudi, M., Groy, T.L., and Yaghi, O.M. (1998). Establishing microporosity in open metal-organic frameworks: gas sorption isotherms for Zn(BDC) (BDC = 1,4-Benzenedicarboxylate). *Journal of the American Chemical Society* 120 (33): 8571–8572.

34 Tranchemontagne, D.J., Mendoza-Cortes, J.L., O'Keeffe, M., and Yaghi, O.M. (2009). Secondary building units, nets and bonding in the chemistry of metal-organic frameworks. *Chemical Society Reviews* 38 (5): 1257–1283.

35 (a) Bragg, W.L. (1914). Die Beugung kurzer elektromagnetischer Wellen durch einen Kristall. *Zeitschrift für Anorganische Chemie* 90 (1): 153–168. (b) Friedrich, W., Knipping, P., and Laue, M. (1913). Interferenzerscheinungen bei Röntgenstrahlen. *Annalen der Physik* 346 (10): 971–988. (c) Komissarova, L.N., Simanov, Y.P., Plyushchev, Z.N., and Spitsyn, V.I. (1966). Zirconium and hafnium oxoacetates. *Russian Journal of Inorganic Chemistry* 11 (9): 2035–2040. (d) Komissarova, L.N.K., Prozorovskaya, S.V., Plyushchev, Z.N., and Plyushchev, V.E. (1966). Zirconium and hafnium oxoacetates. *Russian Journal of Inorganic Chemistry* 11 (2): 266–271. (e) Koyama, H. and Saito, Y. (1954). The crystal structure of zinc oxyacetate, $Zn_4O(CH_3COO)_6$. *Bulletin of the Chemical Society of Japan* 27 (2): 112–114. (f) van Niekerk, J.N., Schoening, F.R.L., and Talbot, J.H. (1953). The crystal structure of zinc acetate dihydrate, $Zn(CH_3COO)_2 \cdot 2H_2O$. *Acta Crystallographica* 6 (8–9): 720–723. (g) van Niekerk, J.N. and Schoening, F.R.L. (1953). X-ray evidence for metal-to-metal bonds in cupric and chromous acetate. *Nature* 171 (4340): 36–37.

36 Lionelle, J.E. and Staffa, J.A. (1983). Metal oxycarboxylates and method of making same. US Patent US10596310.

37 Li, H., Eddaoudi, M., O'Keeffe, M., and Yaghi, O.M. (1999). Design and synthesis of an exceptionally stable and highly porous metal-organic framework. *Nature* 402 (6759): 276–279.

38 (a) Kaye, S.S., Dailly, A., Yaghi, O.M., and Long, J.R. (2007). Impact of preparation and handling on the hydrogen storage properties of

Zn_4O(1,4-benzenedicarboxylate)$_3$ (MOF-5). *Journal of the American Chemical Society* 129 (46): 14176–14177. (b) Tranchemontagne, D.J., Hunt, J.R., and Yaghi, O.M. (2008). Room temperature synthesis of metal-organic frameworks: MOF-5, MOF-74, MOF-177, MOF-199, and IRMOF-0. *Tetrahedron* 64 (36): 8553–8557.

39 Jacoby, M. (2008). Heading to market with MOFs. *Chemical and Engineering News* 86 (34): 13–16.

40 (a) Yaghi, O.M., O'Keeffe, M., Ockwig, N.W. et al. (2003). Reticular synthesis and the design of new materials. *Nature* 423 (6941): 705–714. (b) Kiang, Y.-H., Gardner, G.B., Lee, S. et al. (1999). Variable pore size, variable chemical functionality, and an example of reactivity within porous phenylacetylene silver salts. *Journal of the American Chemical Society* 121 (36): 8204–8215. (c) Jiang, J., Zhao, Y., and Yaghi, O.M. (2016). Covalent chemistry beyond molecules. *Journal of the American Chemical Society* 138 (10): 3255–3265.

Index

Introduction to Reticular Chemistry: Metal-Organic Frameworks and Covalent Organic Frameworks,
First Edition. Omar M. Yaghi, Markus J. Kalmutzki, and Christian S. Diercks.

Companion website: www.wiley.com/go/yaghi/reticular

n